Physics at an Upgraded Fermilab Proton Driver

February 10, 2005

Entire Author list goes here

[1] *First institution*
[2] *Second institution*

DRAFT

Executive Summary

DRAFT

Contents

1 Introduction **3**

2 Neutrino Oscillations **3**
2.1 Oscillation Framework and Measurements 5
2.2 The Importance of the Unanswered Questions 8
2.2.1 The importance of θ_{13} 8
2.2.2 The importance of the Mass Hierarchy 10
2.2.3 The importance of CP Violation and δ 11
2.2.4 The importance of θ_{23} 11
2.3 Evolution of the Global Program 12
2.3.1 The US Accelerator-Based Program 12
2.3.2 The Japanese and European Accelerator-Based Programs . . . 15
2.3.3 Reactor Experiments 16
2.4 Proton Driver Era Sensitivity and the Global Program 16

3 Neutrino Scattering **20**
3.1 Neutrino Scattering Measurements for the Oscillation Program 21
3.2 Neutrino Scattering Physics Program 22
3.3 The Need for a High Intensity Proton Beam at 8 GeV 27

4 The Broader Proton Driver Physics Program **28**
4.1 Muon Physics 29
4.1.1 The Muon Source 30
4.1.2 Electric Dipole Moment 33
4.1.3 Muon g-2 34
4.1.4 Rare Muon Decays 35
4.1.5 Other Muon Experiments 37
4.2 Kaons 37
4.3 Pions 38
4.4 Other Potential Opportunities 41
4.4.1 Neutrons 41
4.4.2 Antiprotons 43

5 Compatibilities and Proton Economics **46**

6 Summary **47**

DRAFT

1 Introduction

In the last few years there has been much interest in a new generation of high intensity multi-GeV proton accelerators capable of delivering a beam of one or a few MW. Recent workshops in Europe, Japan, and the US have explored the physics capabilities and designs for various high-intensity proton source options. The interest in these high-intensity accelerators is driven by the exciting discoveries that have been made in the neutrino sector; namely that neutrinos have mass and that neutrinos of one flavor can transform themselves into neutrinos of a different flavor as they propagate over macroscopic distances. This requires new physics beyond the Standard Model. The scientific case for a Global experimental program to follow up on these recent discoveries and fully explore the neutrino sector is compelling. The recent APS multi-divisional study of the physics of neutrinos concluded that accelerator-based experiments using high-intensity beams and very massive detectors are a critical part of the required Global program, and that the beam intensities that are needed can only be obtained with MW-scale proton sources. Hence, the desired future neutrino oscillation experimental program provides compelling motivation for a new generation of MW-scale proton sources.

Although neutrino oscillations provide the primary motivation for interest in MW-scale proton accelerators, the community participating in recent "Proton Driver" physics workshops has been broader than the neutrino physics community. In particular it has been realized that, as the LHC begins to probe the energy frontier, a new round of precision flavor physics experiments would provide information that is complementary to the LHC data by indirectly probing high mass scales through radiative corrections. This would help to elucidate the nature of any new physics that is discovered at the energy frontier. Should no new physics be discovered at the LHC then, for the foreseeable future, precision muon, pion, kaon, and neutron measurements at a high-intensity proton source may provide the only way to probe physics at mass scales beyond the reach of the LHC. In addition, some high-intensity neutrino scattering and low energy hadron experiments are of interest to the nuclear physics and nuclear astrophysics communities. Hence, a new MW-scale Proton Driver, built primarily to pursue the Global neutrino oscillation physics program, would also offer the possibility of hosting a much broader physics community.

The following describes the physics case for a new 2 MW Proton Driver at Fermilab. Section 2 focuses on neutrino oscillation experiments, and the role that a Fermilab Proton Driver would play in the Global experimental program. Other physics opportunities are discussed in Section 3 (neutrino scattering), and Section 4 (muon, pion, kaon, antiproton, and neutron beams). Compatibilities between the various possible pieces of the experimental program and proton economics are discussed in Section 5.

2 Neutrino Oscillations

Neutrinos are the most ubiquitous matter particles in the universe. In number, they exceed the constituents of ordinary matter (electrons, protons, neutrons) by a factor

of ten billion. They probably account for at least as much energy in the universe as all the stars combined and, depending on their exact masses, might also account for a few percent of the so-called "dark matter". In addition, neutrinos are important in stellar processes. There are about 7×10^{10} cm^{-2} sec^{-1} streaming through the Earth from the Sun. Neutrinos govern the dynamics of supernovae, and hence the production of heavy elements in the universe. Furthermore, if there is CP Violation in the neutrino sector, the physics of neutrinos in the early universe might ultimately be responsible for Baryogenesis. *If we are to understand "why we are here" and the basic nature of the universe in which we live, we must understand the basics properties of the neutrino.*

In the last few years solar, atmospheric, and reactor neutrino experiments have revolutionized our understanding of the nature of neutrinos. We now know that neutrinos produced in a given flavor eigenstate can transform themselves into neutrinos of a different flavor as they propagate over macroscopic distances. This means that, like quarks, neutrinos have a finite mass, the flavor eigenstates are different from the mass eigenstates, and hence neutrinos mix. However, we have incomplete knowledge of the properties of neutrinos since *we do not know the spectrum of neutrino masses, and we have only partial knowledge of the matrix that describes the mixing between the three known neutrino flavor eigenstates.* Furthermore, it is possible that the simplest three-flavor mixing scheme is not the whole story, and that a complete understanding of neutrino properties will require a more complicated framework. In addition to determining the parameters that describe the neutrino sector, the three-flavor mixing framework must also be tested.

The Standard Model cannot accommodate finite neutrino mass terms without some modification. We must either introduce right-handed neutrinos (to generate Dirac mass terms) or allow neutrinos to be their own antiparticle (violating lepton number conservation, and allowing Majorana mass terms). Hence *the physics of neutrino masses is physics beyond the Standard Model.* Although we do not know the neutrino mass spectrum, we do know that the masses, and the associated mass-splittings, are tiny compared to the masses of any other fundamental fermion. This suggests that the physics responsible for neutrino mass will include new components radically different from those of the Standard Model. Furthermore, although we do not have complete knowledge of the neutrino mixing matrix, we do know that it is qualitatively very different from the corresponding quark mixing matrix. The observed difference necessarily constrains our ideas about the underlying relationship between quarks and leptons, and hence models of quark and lepton unification in general, and Grand Unified Theories (GUTs) in particular. Note that in neutrino mass models the seesaw mechanism provides a quantitative explanation for the observed small neutrino masses, which arise as a consequence of the existence of right-handed neutral leptons at the GUT-scale. Over the last few years, as our knowledge of the neutrino oscillation parameters has improved, a previous generation of neutrino mass models has already been ruled out, and a new set of models has emerged specifically designed to accommodate the neutrino parameters. Further improvement in our knowledge of the oscillation parameters will necessarily reject many of these models, and presumably encourage the emergence of new ideas. Hence *neutrino physics is*

experimentally driven, and the experiments are already directing our ideas about what lies beyond the Standard Model.

Our desire to understand both the universe in which we live and physics beyond the Standard Model provides a compelling case for an experimental program that can elucidate the neutrino mass spectrum and mixing matrix, and test the three-flavor mixing framework. It seems likely that complete knowledge of the neutrino mass splittings and of the mixing matrix is accessible to accelerator-based neutrino oscillation experiments. In the following we first introduce the three-flavor mixing framework and identify the critical measurements that need to be made in the future oscillation physics program. The sensitivity of the Fermilab program based on a new 2MW Proton Driver is then considered in the context of the Global experimental program.

2.1 Oscillation Framework and Measurements

We know of three neutrino flavor eigenstates $\nu_\alpha = (\nu_e,\ \nu_\mu,\ \nu_\tau)$. The observed transitions between the flavor eigenstates implies that neutrinos have finite masses, and that the mass eigenstates $\nu_i = (\nu_1,\ \nu_2,\ \nu_3)$ with masses $m_i = (m_1,\ m_2,\ m_3)$ are different from the flavor eigenstates. Within the framework of three-flavor mixing, the mass eigenstates are related to the flavor eigenstates by a 3×3 unitary mixing matrix U^ν,

$$|\nu_\alpha\rangle = \sum_i U^\nu_{\alpha i} |\nu_i\rangle \tag{1}$$

The leptonic charged weak current is given by $J_\lambda = \bar{\nu}_L \gamma_\lambda \ell_L$ where $\ell = (e, \mu, \tau)$, the charged lepton mass eigenstates. The mixing matrix U can be written as

$$U_{\alpha i} = \begin{pmatrix} c_{13}c_{12} & c_{13}s_{12} & s_{13}e^{-i\delta} \\ -c_{23}s_{12} - s_{13}s_{23}c_{12}e^{i\delta} & c_{23}c_{12} - s_{13}s_{23}s_{12}e^{i\delta} & c_{13}s_{23} \\ s_{23}s_{12} - s_{13}c_{23}c_{12}e^{i\delta} & -s_{23}c_{12} - s_{13}c_{23}s_{12}e^{i\delta} & c_{13}c_{23} \end{pmatrix} \tag{2}$$

where $c_{jk} \equiv \cos\theta_{jk}$ and $s_{jk} \equiv \sin\theta_{jk}$. The mixing angles θ_{jk} determine the amplitudes of the neutrino oscillations between the three flavor eigenstates. The complex phase δ determines whether or not neutrino oscillations conserve CP. Note that all of the matrix elements that contain δ also contain a factor s_{13}. Hence, observable CP Violation in the neutrino sector requires that θ_{13} is finite. The frequency of the oscillations is determined by the mass splittings between the mass eigenstates, or more precisely by the $\Delta m^2_{ij} \equiv m^2_i - m^2_j$. In a neutrino oscillation experiment the neutrinos of energy E propagate over a baseline L. A measure of the propagation time is given by L/E, and hence the Δm^2_{ij} will result in oscillations that have maxima at given values of L/E. For experiments with fixed baselines L the energy at which the oscillations occur can be used to determine Δm^2_{ij}, and the amplitudes of the oscillations can be used to determine the mixing angles θ_{ij}. More explicitly, the general neutrino oscillation probability $P_{\alpha\beta} \equiv P(\nu_\alpha \to \nu_\beta) = |\langle\nu_\beta| \exp(-i\mathcal{H}t)|\nu_\alpha\rangle|^2$ in vacuum is given by

$$P_{\alpha\beta} = \left| \sum_{j=1}^{3} U^*_{\alpha j} U_{\beta j} \exp(-iE_j t) \right|^2 = \sum_{j=1}^{3} \sum_{k=1}^{3} U_{\alpha j} U^*_{\alpha k} U^*_{\beta j} U_{\beta k} \exp\left(-i\frac{\Delta m^2_{kj}}{2E} t\right) \tag{3}$$

The existing Global neutrino oscillation data has been used to obtain knowledge of the θ_{ij} and Δm^2_{ij}. In particular:

(i) The Super-Kamiokande [1–3] atmospheric neutrino and K2K [4, 5] accelerator neutrino experiments have shown that muon neutrinos undergo flavor changing transitions whilst propagating over a path length divided by energy (L/E) of the order of $\sim 500\,\mathrm{km/GeV}$. A fit to the data yields $|\Delta m^2_{32}| = (1.5-3.5)\times 10^{-3}\,\mathrm{eV}^2$.

(ii) A fit to the Super-Kamiokande and K2K data also yields the associated oscillation amplitude. In particular $0.35 < \sin^2\theta_{23} < 0.65$ (i.e., $\sin^2 2\theta_{23} > 0.91$). This means the data are consistent with maximal mixing in the (23)-sector. The Super-Kamiokande Collaboration have also reported some supporting evidence that, for the atmospheric neutrino L/E range, muon neutrinos are primarily transformed into tau neutrinos.

(iii) The Super-Kamiokande data shows no significant evidence for muon neutrinos transforming into electron neutrinos. In addition, the CHOOZ [6] reactor experiment has provided tight constraints on electron anti-neutrino transitions for the atmospheric neutrino L/E range, reporting an upper limit on the transition probability of the order of $\sim 5-10\%$. The CHOOZ and Super-Kamiokande experiments have provided a limit on $\sin^2 2\theta_{13}$. The CHOOZ limit is dependent on the input value used for $|\Delta m^2_{31}| \approx |\Delta m^2_{32}|$. For the current central value 2.5×10^{-3} eV^2, the bound is $\sin^2 2\theta_{13} < 0.11$, while for $|\Delta m^2_{31}| = 2.0\times 10^{-3}$ eV^2, it is $\sin^2 2\theta_{13} < 0.18$ [6].

(iv) Together, the Super-Kamiokande, K2K, and CHOOZ data have shown that muon neutrino to tau neutrino transitions occur with large probability when the corresponding L/E is in the atmospheric neutrino range, and that these transitions are well described within the framework of two-flavor neutrino oscillations.

(v) Convincing evidence for neutrino flavor transitions has also been provided by solar neutrino experiments. The SNO [7, 8] experiment has recently shown that solar electron neutrinos transform into muon- and/or tau-neutrinos, and Super-Kamiokande [9] have also shown evidence for solar electron-neutrino flavor transitions. The KamLAND [10] reactor neutrino experiment has confirmed that electron neutrinos "disappear" when propagating over the characteristic L/E scale for solar neutrino transitions. From a combined analysis, the L/E for these flavor transitions is a factor of $\sim$30 times larger than the atmospheric L/E range. A combined analysis of the SNO, Super-Kamiokande, and KamLAND experiments gives $\Delta m^2_{21} = +7.1\pm 2.0\times 10^{-5}\,\mathrm{eV}^2$ and $0.23 < \sin^2\theta_{12} < 0.35$ with $\sin^2\theta_{12} = 0.5$ excluded at more than 5σ. [1] This corresponds to $0.71 < \sin^2 2\theta_{12} < 0.91$.

[1] In fact, more recent global analyzes [11–13] favor a somewhat larger value of $\Delta m^2 = 8.2^{+1.0}_{-0.8}\cdot 10^{-5}\,\mathrm{eV}^2$ (3σ) with much smaller errors.

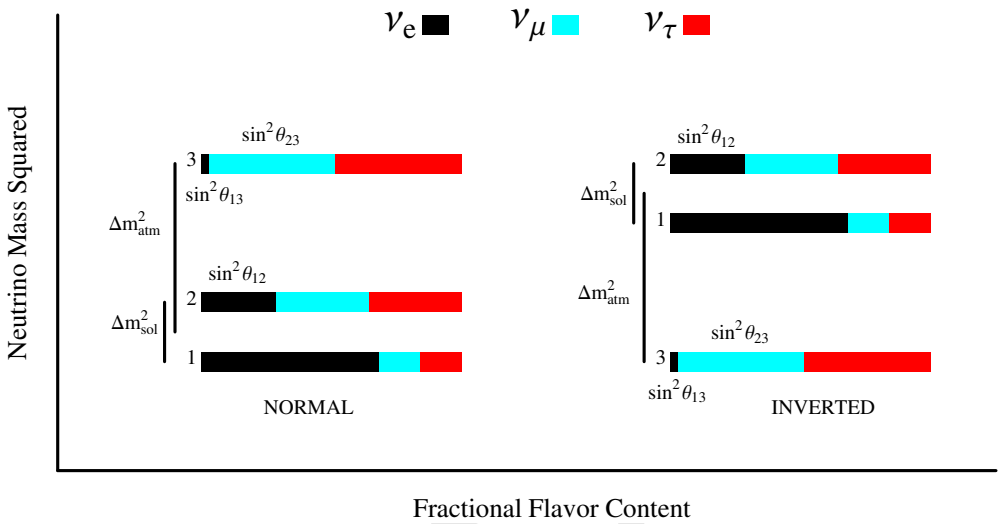

Figure 1: The two allowed three-neutrino mass squared spectra that account for the oscillations of solar and atmospheric neutrinos. The normal spectrum has $\Delta m^2_{32} > 0$ and the inverted has $\Delta m^2_{32} < 0$. The ν_e fraction of each mass eigenstate is indicated by the black solid region whereas the ν_μ (ν_τ) fraction is indicated by the blue (red) regions. The ν_e fraction in the mass eigenstate labeled "3" has been set to the CHOOZ bound.

Together, the atmospheric-, solar-, reactor-, and accelerator-neutrino experiments have shown that all three known neutrino flavors participate in flavor transitions, with two characteristic L/E-ranges, and hence two underlying Δm^2_{ij}. We already have partial knowledge of the Δm^2_{ij} and the mixing angles θ_{ij}. Specifically, we know Δm^2_{21} and the magnitude of Δm^2_{32}. We do not know the sign of Δm^2_{32}. Hence there are two possible patterns of neutrino masses, shown in Fig. 1. The *Normal Hierarchy* corresponds to $\Delta m^2_{32} > 0$, and the *Inverted Hierarchy* corresponds to $\Delta m^2_{32} < 0$. We also have partial knowledge of the mixing angles, and hence the mixing matrix. This knowledge is also summarized graphically in Fig. 1. Specifically, we know approximately θ_{12} and θ_{23}. The measured value of θ_{23}, which describes the amplitude of atmospheric neutrino oscillations, is consistent with maximal mixing, but we don't know if it is really maximal. We have only an upper limit on θ_{13} and no knowledge of the phase δ. To obtain reasonably complete knowledge of the three flavor mixing parameters we need to resolve the ambiguity in the neutrino mass hierarchy, greatly increase the precision of the θ_{23} measurement to determine whether this mixing is close to being maximal, determine θ_{13}, and determine δ.

Finally, it should be noted that there is a possible complication to the simple three-flavor neutrino oscillation picture. The LSND [14] experiment has reported evidence for muon anti-neutrino to electron anti-neutrino transitions for values of L/E which are less than two orders of magnitude smaller than the corresponding values observed for atmospheric neutrinos. The associated transition probability is very small, of the order of 0.3%. If this result is confirmed by the MiniBooNE [15] experiment, it will require a third characteristic L/E range for neutrino flavor transitions. Since each

L/E range implies a different mass-splitting between the participating neutrino mass eigenstates, confirmation of the LSND result would require more than three mass eigenstates. This would be an exciting and radical development. Independent of whether the LSND result is confirmed or not, it is important that the future Global neutrino oscillation program is able to make further tests of the three-flavor oscillation framework.

2.2 The Importance of the Unanswered Questions

Finite neutrino masses require physics beyond the Standard Model (SM). In the most popular candidate theories the SM fermionic field content is supplemented by the introduction of right-handed neutrinos. Since these particles are gauge singlets, their mass scale can be much larger than the electroweak scale, and diagonalization of the resulting mass matrices can yield very small neutrino masses which, in the most economical scheme, are of Majorana type. This "see-saw mechanism" [16–20] can be implemented by embedding the SM into a Grand Unified Theory (GUT) based on a larger gauge symmetry, such as SO(10). Thus, in GUT models the generation of neutrino masses is related to physics close to the GUT scale. Measurements of the neutrino masses and mixings discriminate between GUT models. It should be noted that there are several interesting alternative mechanisms for explaining small neutrino masses. Although these alternative models explain the magnitude of the small neutrino masses using principles similar to the simplest see-saw scheme, they can predict very different phenomenology. See for example Ref. [21–25]. Hence, the determination of the neutrino masses and mixings is expected to yield clues that will help determine whether GUT or other ideas provide a correct description of physics beyond the SM, and help discriminate between the various detailed models.

The basic neutrino oscillation questions that we would like to answer are:

(i) What is the order of magnitude of θ_{13}?

(ii) Is the mass hierarchy Normal or Inverted?

(iii) Is there CP Violation in the neutrino sector and what is the rough value of δ?

(iv) Is θ_{23} (nearly) maximal?

2.2.1 The importance of θ_{13}

Neutrino oscillation experiments have shown that two of the neutrino mixing angles (θ_{23} and θ_{12}) are large. This was a surprise since the equivalent mixing angles in the quark mixing matrix are small. We have only an upper limit on the third neutrino mixing angle θ_{13}. From this limit we know that θ_{13} is much smaller than θ_{23} or θ_{12}. However we have no good reason to expect it to be very small. Predictions from recent models are listed in Table 1. Most of the presently viable neutrino mass models predict that θ_{13} is close to the present bound. A value of θ_{13} much smaller than the bound would suggest a new flavor symmetry that suppresses mixing in the

Model(s)	Refs.	$\sin\theta_{13}$	$\sin^2 2\theta_{13}$
Minimal SO(10)	[26]	0.18	0.13
Orbifold SO(10)	[27]	0.1	0.04
SO(10) + Flavor symmetry	[28]	$5.5 \cdot 10^{-4}$	$1.2 \cdot 10^{-6}$
	[29]	0.014	$7.8 \cdot 10^{-4}$
	[30–32]	0.05 .. 0.1	0.01 .. 0.04
	[33–35]	0.15 .. 0.22	0.09 .. 0.18
SO(10) + Texture	[36]	0.01 .. 0.06	$4 \cdot 10^{-4}$ .. 0.01
	[37]	0.1	0.04
$SU(2)_L \times SU(2)_R \times SU(4)_c$	[38]	0.15	0.09
Flavor symmetries	[39–41]	0	0
	[42–44]	$\lesssim 0.03$	$\lesssim 0.004$
	[45–47]	0.005 .. 0.07	10^{-4} .. 0.02
	[44, 48–51]	0.1 .. 0.2	0.04 .. 0.15
Textures	[52]	0.01 .. 0.05	$4 \cdot 10^{-4}$ .. 0.01
	[53–56]	0.08 .. 0.2	0.03 .. 0.15
3×2 see-saw	[57]	0.1	0.04
	[58] (n.h.)	0.07	0.02
	(i.h.)	> 0.006	$> 1.6 \cdot 10^{-4}$
Anarchy	[59]	> 0.1	> 0.04
Renormalization group enhancement	[60]	0.08 .. 0.1	0.03 .. 0.04
M-Theory model	[24]	0.005	10^{-4}

Table 1: Selection of predictions for θ_{13}. The numbers should be considered as order of magnitude statements. The abbreviations "n.h." and "i.h." refer to the normal and inverted hierarchies, respectively.

(13)-sector. However, even if this is the case and θ_{13} is exactly zero at the GUT scale, radiative corrections would be expected to drive its value away from zero at laboratory energies, yielding a non-zero measured value. The size of these quantum effects can be estimated using the differential equations derived in Ref [61] (see also Refs [62, 63] for related works). The radiative corrections are negligible in the SM due to the smallness of the charged lepton Yukawa couplings. In the MSSM (Minimal Supersymmetric Standard Model), they are enhanced by $\tan\beta$, the ratio of the two Higgs vacuum expectation values. In addition to the oscillation parameters and $\tan\beta$, the running depends on the mass of the lightest neutrino and the value of the Majorana CP phases in the lepton mixing matrix. The estimated change of $\sin^2 2\theta_{13}$ in the MSSM is shown in Figure 2. The shift is larger than 0.01 for a considerable parameter range. The viable parameter range becomes very restricted if $\sin^2 2\theta_{13}$ is less than O(0.001). Hence, if θ_{13} is determined to be much smaller than the present bound we may suspect a new lepton flavor symmetry. If θ_{13} is extremely small, such that $\sin^2 2\theta_{13} << 0.001$ for example, its value may place the GUT concept under pressure. In any case *determining the order of magnitude of θ_{13} will provide crucial guidance toward an understanding of the physics of neutrino masses.*

In addition to its theoretical importance, the order of magnitude of θ_{13} has impor-

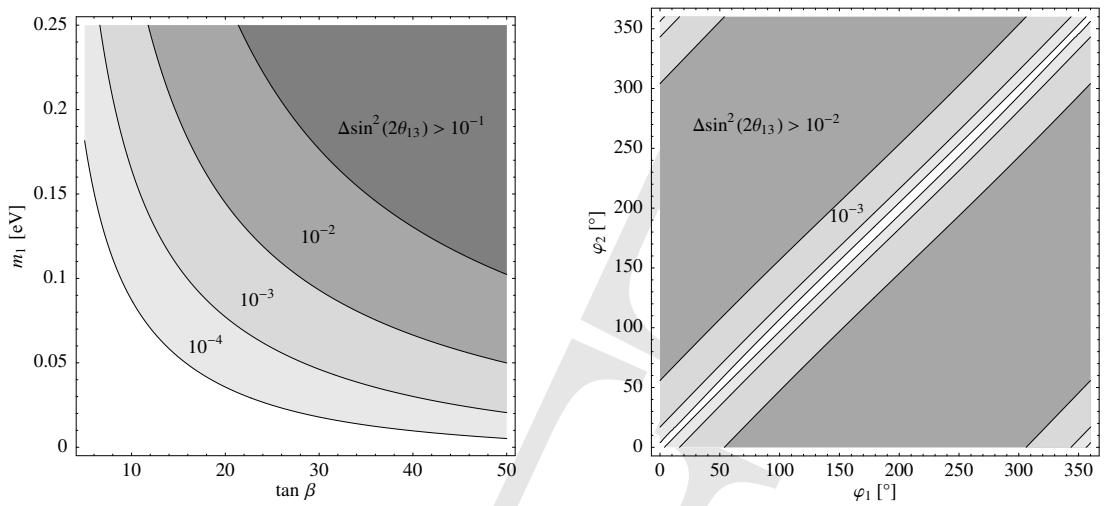

Figure 2: Corrections to θ_{13} from the running between 10^2 and 10^{12} GeV in the MSSM, calculated using the initial conditions $\theta_{13} = 0$ and best-fit values for the remaining parameters, as well as a normal mass hierarchy. In the left figure, the corrections are shown as a function of $\tan\beta$ and m_1, the mass of the lightest neutrino (with Majorana phases $\varphi_1 = 0$ and $\varphi_2 = \pi$). The right plot illustrates the dependence on the Majorana CP phases φ_1 and φ_2 (as defined in Ref [61]) for $\tan\beta = 50$ and $m_1 = 0.08$ eV. The contour lines are defined as in the left diagram. (Plots taken from Ref [61].)

tant experimental consequences. If θ_{13} is within an order of magnitude of its present bound we may know its value before the "Proton Driver Era". A Proton Driver would then enable the mass hierarchy to be determined and a search for CP violation to be made. If θ_{13} is between one and two orders of magnitude of the present bound we will probably not know its value before the Proton Driver Era. The Proton Driver program would then greatly improve our knowledge of θ_{13}, and perhaps determine the mass hierarchy, but would not be sufficiently sensitive to pin down δ and make a sensitive search for CP Violation. In this scenario a Proton Driver would, however, prepare the way for the ultimate neutrino oscillation tool, a Neutrino Factory, if required. Hence, *the value of θ_{13} will determine which facilities and experiments will be needed beyond the initial Proton Driver experiments to complete the neutrino oscillation program.* The θ_{13} sensitivity is discussed in more detail in Section 2.4.

2.2.2 The importance of the Mass Hierarchy

Specific neutrino mass models are usually only compatible with one of the two possible neutrino mass hierarchies (normal or inverted). A measurement of the sign of Δm^2_{31} would therefore discriminate between models. For example, GUT models with a standard type I see-saw mechanism tend to predict a normal hierarchy (see, for example, the reviews Refs [64, 65]), while an inverted hierarchy is often obtained in models that employ flavor symmetries of such as $L_e - L_\mu - L_\tau$ [66, 67].

A determination of the sign of Δm^2_{31} would also have some consequences for neutrinoless double beta decay experiments. A negative Δm^2_{31} would imply a lower limit on the effective mass for neutrinoless double beta decay (in the case of Majorana neutrinos) which would be expected to be within reach of the next generation of

Model(s)	Refs.	$\lvert 0.5 - \sin^2\theta_{23}\rvert$
Minimal SO(10)	[26]	> 0.16
SO(10) + Flavor symmetry	[29, 30, 72]	$\lesssim 0.05$
SO(10) + Texture	[36]	$\lesssim 0.11$
Flavor symmetries	[39, 40, 48, 49, 73–75]	0
	[42]	0.02
	[76]	0.04
	[47]	0.04 .. 0.1
	[43, 44]	$\gtrsim 0.07$
Sequential RH neutrino dominance	[77–79]	0.1
+ Flavor symmetries	[31, 50, 80]	0.1
+ Type II see-saw upgrade	[45]	0.01 .. 0.1
Texture zeros	[52]	0.07
	[81]	> 0.1
Perturbations of textures	[82]	$\lesssim 0.16$
	[83, 84]	0.005 .. 0.1
M-Theory model	[24]	0.02

Table 2: Selection of theoretical expectations for $\lvert 0.5 - \sin^2\theta_{23}\rvert$ at tree level. The numbers should be considered as order of magnitude statements.

experiments.

2.2.3 The importance of CP Violation and δ

Leptogenesis [68], in which CP Violation in the leptonic Yukawa couplings ultimately results in a baryon asymmetry in the early Universe, provides an attractive possible explanation for the observed baryon asymmetry. In the most general case, the CP phases involved in leptogenesis are not related to the low-energy CP phases that appear in the effective neutrino mass matrix [69, 70]. However, specific neutrino mass models can yield relationships between the CP violation relevant to leptogenesis and the low-energy CP phases. Examples are models in which flavor symmetries and texture zeros restrict the structure of the coupling matrices. In these models, to successfully obtain leptogenesis typically requires a non-zero Dirac phase δ (see, for example, Refs [57, 71]). Hence, although a measurement of CP Violation in the neutrino sector would not establish leptogenesis as the right explanation for the observed baryon asymmetry, it would be suggestive. Furthermore, the measured value of δ would help discriminate between the various neutrino mass models that successfully predict the observed baryon/photon ratio.

2.2.4 The importance of θ_{23}

Atmospheric neutrino experiments have shown that θ_{23} is large and is consistent with $\theta_{23} = \pi/4$, corresponding to maximal mixing in the (23)-sector. Predictions for θ_{23} from a variety of presently viable neutrino mass models are listed in Table 2. A

precise measurement of θ_{23} would discriminate between the models. Note that there are models where the predicted θ_{23} lies in a range that does not include maximal mixing [26, 31, 43, 44, 47, 81]. In many other cases, although a large atmospheric angle can be accommodated, almost maximal mixing would require some tuning (see for example Refs [34, 36, 37, 51, 60, 85–87]). In other cases a value of θ_{23} rather close to $\pi/4$ is predicted at leading order, but various sources cause deviations from $\pi/4$ that would typically be detectable by future experiments (see for example Refs [27, 29, 30, 72]). A measured value of θ_{23} very close to $\pi/4$ would suggest a new underlying symmetry, and would place a strong constraint on neutrino mass models.

2.3 Evolution of the Global Program

In the coming years we can expect improvements in our knowledge of the oscillation parameters from the present generation of running experiments (MiniBooNE, KamLAND, K2K, MINOS) and experiments under construction (T2K). Beyond this a new generation of reactor and accelerator based experiments are being proposed (for example the Double-CHOOZ reactor experiment and the NpνA experiment using the NuMI beam). In the following we describe the expected evolution of our knowledge over the next decade. It should be noted that the present neutrino oscillation program is fully Global in its character, with the various regions hosting complementary experiments. A list of relevant experiments and their characteristics is given in Table 3. The $\sin^2 2\theta_{13}$ sensitivities for these experiments are summarized in Fig 3, where the other oscillation parameters have been chosen to correspond to the present central values. The dependence of the $\sin^2 2\theta_{13}$ sensitivities on Δm^2_{31} is shown in Fig. 4. Clearly, as our knowledge of Δm^2_{31} improves the estimated θ_{13} sensitivities will become more precise. The $\sin^2 2\theta_{23}$ sensitivities for the experiments is summarized in Table 4.

2.3.1 The US Accelerator-Based Program

In the US there are two approved neutrino oscillation experiments, both hosted by Fermilab.

The MiniBooNE experiment is designed to test the neutrino oscillation interpretation of the LSND data. MiniBooNE is presently data taking, and is expected to deliver its central result in about a year. If this result is positive the long-baseline neutrino oscillation experiments will continue to be important, but the emphasis within the oscillation program will almost certainly shift to focus on the new discovery. High intensity experiments at MW-scale proton drivers will very likely play a pivotal role in exploring the new physics that will emerge in this exciting scenario. The MiniBooNE result will define a major branch point in the Global neutrino physics road map. In the following we will assume a negative result. If this is not the case, in about a year from now we would expect a reevaluation of the neutrino physics roadmap based on the MiniBooNE measurements.

MINOS is a muon-neutrino disappearance experiment that is expected to confirm the oscillation interpretation of the atmospheric neutrino data and to better determine

Label	L	$\langle E_\nu \rangle$	P_{Source}	Detector technology	m_{Det}	t_{run}
Conventional beam experiments:						
MINOS	735 km	3 GeV	$3.7 \cdot 10^{20}$ pot/y	Magn. iron calorim.	5.4 kt	5 yr
ICARUS	732 km	17 GeV	$4.5 \cdot 10^{19}$ pot/y	Liquid Argon TPC	2.35 kt	5 yr
OPERA	732 km	17 GeV	$4.5 \cdot 10^{19}$ pot/y	Emul. cloud chamb.	1.65 kt	5 yr
Superbeams:						
T2K	295 km	0.76 GeV	$1.0 \cdot 10^{21}$ pot/y	Water Cherenkov	22.5 kt	5 yr
NOνA†	812 km	2.22 GeV	$4.0 \cdot 10^{20}$ pot/y	Low-Z-calorimeter	50 kt	5 yr
Reactor experiments:						
D-Chooz†	1.05 km	~ 4 MeV	2×4.25 GW	Liquid Scintillator	11.3 t	3 yr
Reactor-II†	1.70 km	~ 4 MeV	8 GW	Liquid Scintillator	200 t	5 yr
Short Baseline experiments:						
MiniBooNE	0.54 km	0.7 GeV	$3 \cdot 10^{20}$ pot/y	Oil Cherenkov	450 t	3 yr

† proposed

Table 3: The different classes of experiments and the considered setups. The table shows the label of the experiment, the baseline L, the mean neutrino energy $\langle E_\nu \rangle$, the source power P_{Source} (for beams: in protons on target per year, for reactors: in gigawatts of thermal reactor power), the detector technology, the fiducial detector mass m_{Det}, and the running time t_{run}. Note that most results are, to a first approximation, a function of the product of running time, detector mass, and source power. Table modified from Ref [88].

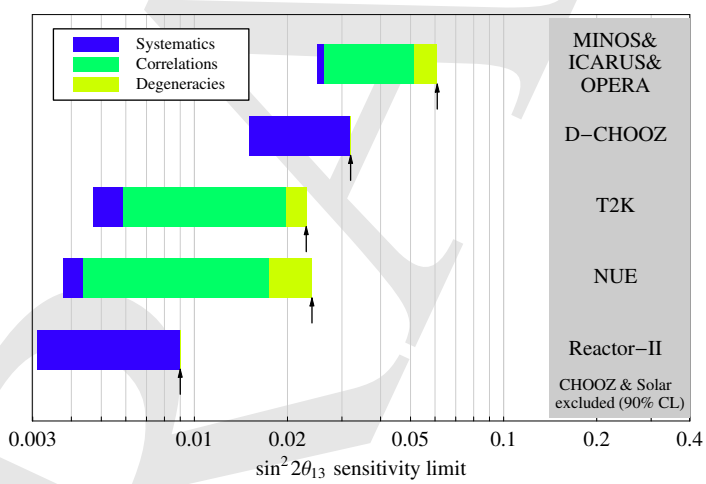

Figure 3: The $\sin^2 2\theta_{13}$ sensitivity limit at the 90% CL for MINOS, ICARUS, and OPERA combined, Double-Chooz, T2K, Reactor-II , and a NuMI Upgraded Experiment (NUE). Note that for the calculation NUE corresponds to the proposed NOνA experiment (see Table 3). The left edges of the bars are obtained for the statistics limits only, whereas the right edges are obtained after successively switching on systematics, correlations, and degeneracies, *i.e.*, they correspond to the final $\sin^2 2\theta_{13}$ sensitivity limits. The gray-shaded region corresponds to the current $\sin^2 2\theta_{13}$ bound at 90% CL. For the true values of the oscillation parameters, we use $|\Delta m^2_{31}| = 2.0 \cdot 10^{-3}\,\text{eV}^2$, $\sin^2 2\theta_{23} = 1$, $\Delta m^2_{21} = 7.0 \cdot 10^{-5}\,\text{eV}^2$, $\sin^2 2\theta_{12} = 0.8$ [8, 89–91], and a normal mass hierarchy. Figure extended version from Ref. [88].

the associated $|\Delta m^2|$. MINOS will also have some capability to detect electron-neutrino appearance, and hence has some sensitivity to θ_{13}. However, this sensitivity

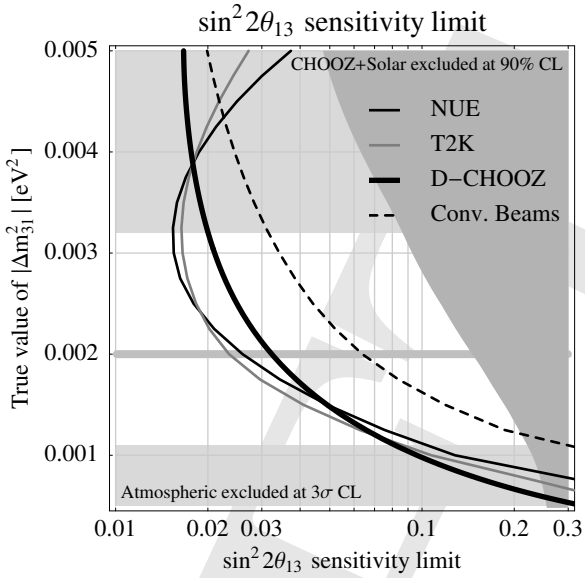

Figure 4: The $\sin^2 2\theta_{13}$ sensitivity limits at 90% CL from the experiments NUE, T2K, Double-Chooz, and the combined conventional beams (MINOS, ICARUS, OPERA) as function of the true value of $|\Delta m^2_{31}|$. The dark-gray shaded region refers to the current $\sin^2 2\theta_{13}$ bound from CHOOZ and the solar experiments (90% CL) [90].Same parameter values as in Figure 3. Figure taken from Ref [88].

Experiment/Combination	$\lvert\Delta m^2_{31}\rvert$	θ_{23}	$\sin^2\theta_{23}$
MINOS + OPERA + ICARUS	$2^{+0.34}_{-0.18}\cdot 10^{-3}\,\mathrm{eV}^2$	$(\pi/4)^{+0.22}_{-0.19}$	$0.5^{+0.21}_{-0.18}$
T2K	$2^{+0.15}_{-0.09}\cdot 10^{-3}\,\mathrm{eV}^2$	$(\pi/4)^{+0.13}_{-0.10}$	$0.5^{+0.13}_{-0.10}$
NUE	$2^{+0.43}_{-0.07}\cdot 10^{-3}\,\mathrm{eV}^2$	$(\pi/4)^{+0.24}_{-0.21}$	$0.5^{+0.23}_{-0.20}$
All beam experiments combined	$2^{+0.12}_{-0.06}\cdot 10^{-3}\,\mathrm{eV}^2$	$(\pi/4)^{+0.13}_{-0.10}$	$0.5^{+0.12}_{-0.09}$

Table 4: The expected allowed ranges (3σ, 1 d.o.f.) for the atmospheric oscillation parameters. For the true values of the oscillation parameters, we choose the same values as in Figure 3. The impact of an inverted mass hierarchy, and different values for $\sin^2 2\theta_{13}$ or δ_{CP} on these final results is rather small. Table taken from Ref [88].

is limited. MINOS is just beginning to start data taking. In the coming 5 years we expect MINOS to determine θ_{13} if it is very close to the present bound. MINOS is also expected to reduce the uncertainty on $|\Delta m^2_{31}|$ to about $\pm 10\%$.

Looking further into the future, significant progress could be made with a new long-baseline experiment that exploits the NuMI beamline, together with an upgraded Proton Driver, and a detector that is optimized to detect ν_e appearance. In the following we will refer to this generic NuMI Upgraded Experiment as NUE. There are several possible detector technology choices for NUE. There are also choices for the central beam energy and baseline, which are related to choices about whether the detector is on-axis (with respect to the central beam direction) or off-axis. Some examples of possible beam spectra are shown in Fig. 5. In the following we have exploited the calculations available from the NOνA collaboration to obtain a quanti-

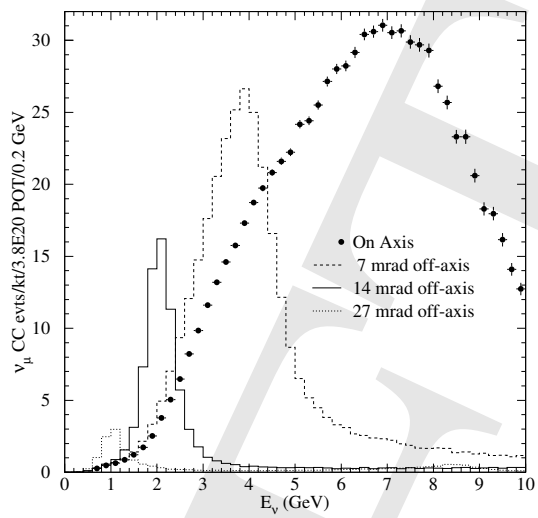

Figure 5: Event rates at various off axis angles with respect to the NuMI beamline, for the medium energy configuration.

tative understanding of the achievable sensitivity at a 2 MW Proton Driver. Hence, NUE numbers and figures in the following discussion correspond to a 50 kt detector placed about 15 mrad off-axis from the NuMI beamline, and a baseline of 812 km. Although no NuMI upgraded experiment has yet been approved, we might imagine that NOνA, or an equivalent experiment, is approved, constructed, and becomes operational in 5-10 years from now. Based on NOνA calculations, after 5 years of data taking we would expect NUE to determine $\sin^2 2\theta_{13}$ if it exceeds ~ 0.02.

2.3.2 The Japanese and European Accelerator-Based Programs

K2K was designed to provide the first accelerator-based test of atmospheric neutrino oscillations. K2K has just finished data taking. This experiment has already provided an accelerator-based confirmation of the atmospheric neutrino oscillation parameters. Although the data analysis continues, we anticipate only an incremental further improvement in our knowledge from the remaining analysis.

In Europe, the CNGS program consists of two experiments, ICARUS and OPERA, designed to study tau-neutrino appearance with an L/E corresponding to the atmospheric neutrino oscillation scale. In addition, there will be sensitivity to electron-neutrino appearance, and hence to θ_{13}. The CNGS experiments are expected to begin running in a few years. After 5 years of data taking, the combined sensitivity of ICARUS, OPERA, and MINOS will enable $\sin^2 2\theta_{13}$ to be determined if it exceeds ~ 0.06.

In Japan the beamline for T2K, a high-statistics, off-axis, second generation version of K2K, has been approved, and is expected to be completed in 2009. With 5 years of data taking T2K is expected to determine $\sin^2 2\theta_{13}$ if it exceeds ~ 0.02. The

combined NUE and T2K sensitivity would be in the range 0.01-0.02.

2.3.3 Reactor Experiments

A new generation of reactor experiments are being proposed with detectors and baselines chosen to be sensitive to θ_{13}. Although choices still have to be made to determine which of these experiments are supported, it seems reasonable to assume that one or two reactor experiments will be executed in the coming decade. The Double-CHOOZ experiment appears to be furthest along in the approval process. This experiment is expected to determine $\sin^2 2\theta_{13}$ if it exceeds ~ 0.03. Beyond this, a more ambitious reactor experiment, referred to in Table 3 as Reactor II, might be expected to reach a sensitivity $\sin^2 2\theta_{13}$ approaching 0.01. This sensitivity is slightly better than the corresponding sensitivity expected for T2K, and might be obtained on a similar timescale.

2.4 Proton Driver Era Sensitivity and the Global Program

In the following we begin by considering the sensitivity that could be achieved with a 2 MW MI proton beam and a first generation electron-neutrino appearance detector using the existing NuMI beamline. We also consider how the Fermilab program fits within the Global neutrino program, and how both might evolve in the longer term. The anticipated evolution of the $\sin^2 2\theta_{13}$ sensitivity of the Global neutrino oscillation program is illustrated in Fig. 6. The sensitivity in expected to improve by about an order of magnitude over the next decade. This progress is expected to be accomplished in several steps, each yielding a factor of a few increased sensitivity. During this first decade the Fermilab program will have contributed to the improving Global sensitivity with MINOS, followed by NUE. MINOS is the on-ramp for the US long-baseline neutrino oscillation program. NUE would be the next step. Note that we assume that NUE starts data taking with the existing beamline before the Proton Driver era. The Proton Driver would take NUE into the fast lane of the Global program.

At the end of the decade the Global $\sin^2 2\theta_{13}$ sensitivity is anticipated to be ~ 0.01. Hence, if $\sin^2 2\theta_{13} > 0.01$ we will know its value before the Proton Driver era, and the Global program will be focused on determining the neutrino mass hierarchy, searching for CP Violation, and making precision measurements of the oscillation parameters. The evolution of the Global sensitivities to the neutrino mass hierarchy and to CP Violation in the neutrino sector are illustrated in Fig. 7. If $\sin^2 2\theta_{13} > 0.01$ then NUE at an upgraded Proton Driver would enable the mass hierarchy to be determined for much of the viable parameter space (left panel of Fig. 7) and a first search to be made for CP Violation over a limited region of parameter space (right panel of Fig. 7). Note that if the T2K experiment was also upgraded (T2K*), the combined NUE+PD+T2K* sensitivity would enable the mass hierarchy to be determined for almost the entire parameter space, and the search for CP Violation to be significantly improved. Hence, the existence of a first generation Fermilab Proton Driver experiment would make an upgrade to the T2K experiment very attractive. With

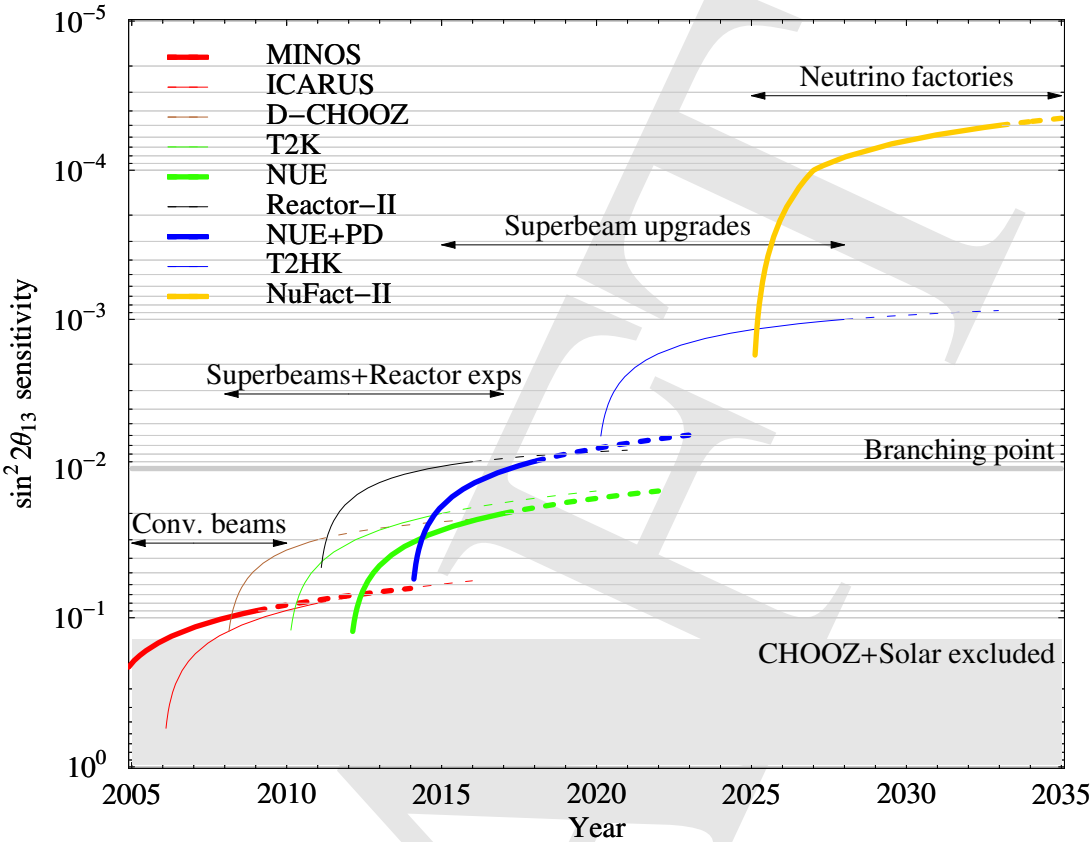

Figure 6: Anticipated evolution of the $\sin^2 2\theta_{13}$ sensitivity of the Global neutrino program. The final sensitivities for each sub-program (right ends of solid curves) and the guesstimated data taking periods are taken from Refs. [88,92,93], and correspond to the results from detailed simulations. The dashed curves indicate possible extensions of the sub-programs. The thick curves represent a possible Fermilab program. The "branching point" at $\sin^2 2\theta_{13} = 0.01$ shows the point at which a decision can be made for an upgraded Global superbeam program. The choices include additional NUE detectors (possibly a very large water Cherenkov detector), a new beamline, and a Neutrino Factory. Note that although we have chosen the starting times of the experiments as close as possible as stated in the respective LOIs, they have to be interpreted with care. For the Japanese program, we assume that the upgrade T2HK will start ten years after T2K starts, and for the neutrino factory, we assume a starting time ten years after the branching point is reached. For the time-scaling of the sensitivity limits, we assume a simplified background dominated scaling $\propto \sqrt{N}$ in almost all cases except for the neutrino factory, which in the absence of background scales with $\propto N$ for $\sin^2 2\theta_{13} \lesssim 10^{-4}$. For the reactor experiments and T2HK , we in addition assume a systematics limitation in the extensions (which corresponds to a large uncorrelated bin-to-bin error for the reactor experiments).

two very different baselines NUE and T2K* are complementary and when combined provide enough experimental input to uniquely determine the oscillation parameters over a significant region of parameter space. In the longer term, if the first generation experiment(s) failed to establish the mass hierarchy and/or CP Violation, there are alternative upgrade paths in which the NUE detector mass is increased (SNUE), or

a second off-axis detector with a different baseline is added, or a new longer-baseline beamline is built, and/or the Japanese program includes a megaton-class detector (T2HK). Which option is optimal for the Fermilab contribution to the Global program will depend on both results from the first generation experiments and decisions about how the Japanese and European programs evolve.

If $\sin^2 2\theta_{13}$ is less than ~ 0.01 we will not know its value before the Proton Driver experiment begins data taking. The Global program will be focused on significantly improving the $\sin^2 2\theta_{13}$ sensitivity, and preparing for a Neutrino Factory which will ultimately be needed to make progress. Hence, in about a decade we anticipate reaching a branch point at which time the need for a Neutrino Factory can be assessed. If we imagine the decision-making and construction time for a Neutrino Factory is about a decade, then in the second decade from now NUE at a Proton Driver, perhaps enhanced with a modest upgrade, would improve the $\sin^2 2\theta_{13}$ sensitivity by a factor of a few. We note that the path the Global neutrino program will take beyond the $\sin^2 2\theta_{13} \sim 0.01$ branch point, and the role of the Fermilab program, will be influenced by the NUE+PD result, the experience gained operating the PD (Note: A PD is also needed for a Neutrino Factory), and progress with Neutrino Factory R&D.

Finally, the NUE sensitivities discussed so far have used results from calculations made for the proposed NOvA detector placed off-axis from the NuMI beamline. An alternative approach has been proposed by the Brookhaven group which uses a massive water Cherenkov detector on axis in a broadband beam with a longer baseline. In addition to a Proton Driver upgrade this will require a new beamline and a very large detector presumably sited in a new underground laboratory. The advantage of the broadband beam scenario is that the broad energy spectrum would enable the detailed neutrino spectrum to be measured covering two, or possibly three, of the oscillation maxima. This would provide good sensitivity to both matter effects and CP Violation. The calculated sensitivity depends upon what is assumed for the backgrounds that must be subtracted from the electron-neutrino appearance signal, and in particular the background from NC events at higher energies that feed down into the low energy signal region. It should be noted that although the Brookhaven group have calculated the signal sensitivity that might be obtained using an upgraded AGS and a beam pointing from BNL to the Homestake mine ($L = 2540$ km), the scheme is in general laboratory-independent, although the possible choices for the baseline are not. Calculations have therefore been made for a broadband beam and a baseline corresponding to Fermilab to Homestake ($L = 1290$ km). The precision that might be obtained in the $(\sin^2 2\theta_{13}, \delta_{CP})$-plane is shown in Fig. 8. A Fermilab to Homestake broadband experiment would appear to be a competitive alternative to the BNL-Homestake proposal. This might therefore be a possible upgrade of the Fermilab neutrino program beyond the $\sin^2 2\theta_{13} \approx 0.01$ branch point, at which time we will expect to have have further knowledge of ν_e appearance backgrounds from the T2K running. It should be noted that one variant to the broadband beam scheme that has been proposed for a second generation Proton Driver experiment would utilize the 8 GeV Proton Driver beam to create a low energy neutrino beam that is sent to the same long-baseline detector as the MI NuMI beam. This would enable a broad neutrino energy spectrum to be spanned by a number of narrow-band beams; a

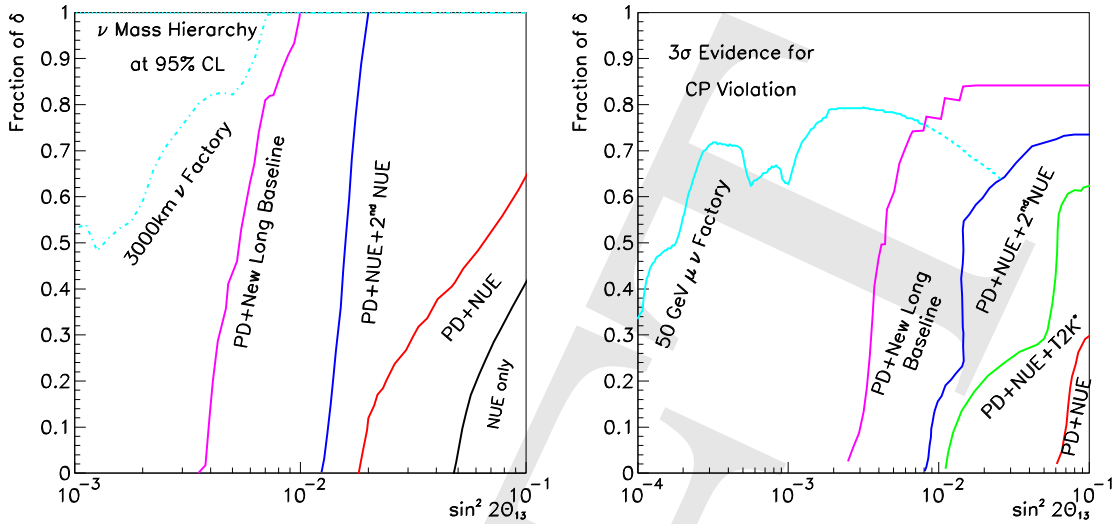

Figure 7: Possible evolution of the experimental sensitivity to the neutrino mass hierarchy (left plot) and CP violation in the lepton sector (right plot). The sensitivity is characterized by, for each value of $\sin^2 2\theta_{13}$, the fraction of the δ parameter space for which the mass hierarchy could be determined at 2σ or CP violation observed at 3σ. Note that δ is the unknown CP phase in the mixing matrix. The curves correspond to various stages of the global neutrino oscillation program. 'NUE alone" corresponds to a 50kton NUE detector at 15 mrad from the NuMI beamline axis running 3 years neutrino mode, 3 years antineutrino mode, with a 0.4 MW proton source. "PD+NUE" corresponds to the same running time and detector but with 2 MW proton driver. PD+NUE+T2K* corresponds to the addition of T2K with an upgraded proton source (4 MW), with the same 3+3 year run. "PD+NUE + $2^{\rm nd}$NUE" corresponds to the addition of a 50kton detector at 42mrad, where the new (later) detector runs for 3+3 years, and the 15 mrad detector takes data for 6+6 years. PD+new long baseline or T2HK corresponds to either a new long baseline ($> 1000\ km$) experiment combined with a Megaton class detector (at a National Underground Lab), or combining PD+NUE + T2K with the Hyper-Kamiokande detector. The Neutrino Factory consists of a 50GeV muon storage ring with 5×10^{20} muon decays per year, fed by a 4MW proton source, with 4ν+$4\bar{\nu}$ years of running time and a 50 kton MINOS-like detector. (NUE curves provided by the NOνA collaboration).

capability that would be unique to the Fermilab Proton Driver complex. The advantage of this scheme is that the first, second, and possibly third oscillation maximum can be measured whilst backgrounds from the unwanted high-energy tail inherent in a broad-band beam can be suppressed or eliminated. If this scheme was favored it would motivate the highest intensity 8 GeV proton beam practical, and hence motivates an 8 GeV Proton Driver design with an upgrade path to a beam power of 2 MW or more.

To summarize, we envision a Global neutrino road map in which there are a number of branch points, but in each case a neutrino program based on an upgraded Fermilab Proton Driver will play a pivotal role. Within the US, the newly constructed NuMI beamline provides the onramp for this longer term program. The first generation Proton Driver experiment, NUE, is common to all routes on the road map and, together with a new Proton Driver, will take the US neutrino program into the fast lane of the Global program. In about a decade from now our knowledge of $\sin^2 2\theta_{13}$

DRAFT

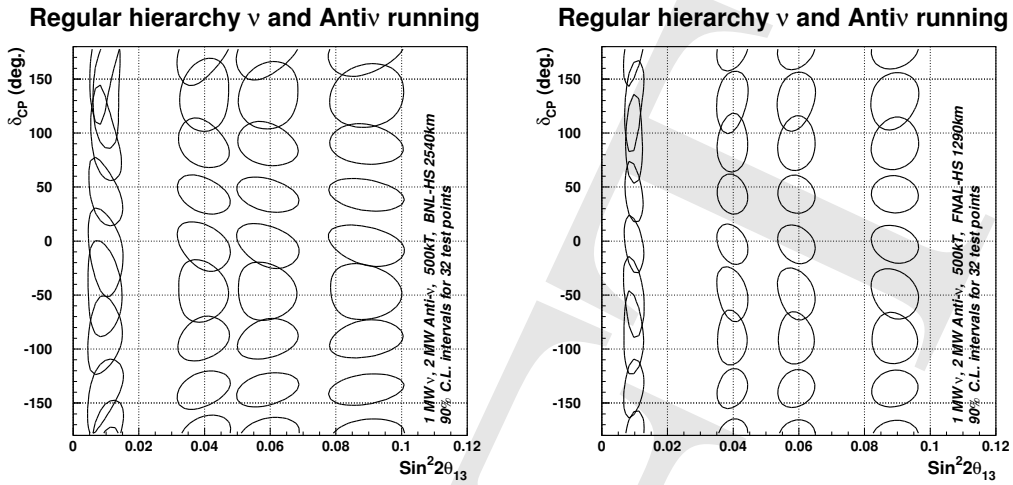

Figure 8: 90% confidence level error contours in $\sin^2 2\theta_{13}$ versus δ_{CP} for statistical and systematic errors for 32 test points. This simulation is for combining both neutrino and anti-neutrino data. Left is for BNL-HS and right is for FNAL-HS. We assume 10% systematic errors for this plot. Figure taken from Ref. [94].

will have reached the 0.01 branch point, and a decision about the second generation Proton Driver experiment(s) versus a Neutrino Factory can be made. Results from reactor experiments and the first generation NUE experiment, together with results from T2K and from continued Neutrino Factory R&D, will guide the decision.

3 Neutrino Scattering

Fermilab is the host laboratory for the US accelerator based neutrino program. With the recent approval of the MINERνA Experiment, the US accelerator-based neutrino program will include a program of high-statistics neutrino scattering measurements. These measurements are of interest to a broad community of particle physicists, nuclear physicists, and nuclear astrophysicists. More precise neutrino cross-section measurements are also needed to reduce the otherwise dominant systematic uncertainties on the measurements of precise neutrino oscillation parameters. The MINERνA experiment will enable precise measurements of neutrino scattering on nuclear targets, but the statistical precision will not be sufficient to obtain precise measurements of neutrino scattering on nucleon targets (hydrogen and deuterium), or precise measurements of antineutrino scattering. The antineutrino event rates are, depending on energy, a factor of 3 - 5 less than the neutrino rates per proton on target. The interaction rates on nucleon targets are an order of magnitude less than the corresponding interaction rates with nuclear targets. Hence, to obtain precise neutrino and antineutrino-nucleon as well as antineutrino-nucleus measurements a factor of $10 - 100$ increase in data rates will be required. An upgraded Proton Driver delivering 2 MW beam power at both MI energies and at 8 GeV, together with neutrino

scattering detectors a factor of a few more massive than MINERνA, would provide the needed data samples.

3.1 Neutrino Scattering Measurements for the Oscillation Program

To measure neutrino oscillation probabilities it is necessary to know the composition, intensity, divergence, and energy spectrum of the initial beam, and also know all the relevant neutrino and antineutrino cross-sections as well as the important nuclear effects for interactions in the absorber material of the far detector. A well designed "near detector" enables the initial beam to be well characterized, and provides cross-section measurements with adequate precision for the oscillation program. In practice it has proved necessary to have more than one type of near detector. The K2K Experiment used both a near detector that replicated the far detector, and additional near detectors optimized to learn more about the underlying cross-sections. The Fermilab long baseline neutrino program is following a similar strategy. The MINOS near detector replicates the far detector, and the MINERνA detector has been designed to learn more about the underlying cross-sections and nuclear effects.

As neutrino oscillation data samples increase there will be a corresponding need to improve the precision of the near detector measurements. In particular we know that the all-important $\nu_\mu \to \nu_e$ oscillations driven by the atmospheric-neutrino Δm^2 has an associated oscillation amplitude of at most 5%. Hence, it is particular important to determine, with a precision of a fraction of a percent, the neutrino cross-sections for all the potential background processes. As a quantitative example of how neutrino scattering measurements are essential for $\nu_\mu \to \nu_e$ experiments, consider how the MINERνA experiment would help the proposed NOνA experiment. A preliminary quantitative study [95] has been performed. Figure 9 shows the statistical and systematic error on $\sin^2 2\theta_{13}$ for NOνA as a function of $\sin^2 2\theta_{13}$. Two different systematic uncertainties are shown: one assuming the current cross-section uncertainties, the other assuming the reduced uncertainties expected as a result of MINERνA.

These preliminary studies illustrate how neutrino scattering experiments will play a key role in allowing future precision oscillation experiments to reach their ultimate sensitivity. To obtain the most precise value of Δm^2_{23} (which is eventually required to extract mixing angles and the CP-violating phase) we must better understand and quantify the nuclear processes interposed between the interaction of an incoming neutrino and measurement of outgoing particles in the detector. Extracting mixing parameters such as θ_{13}, and ultimately the neutrino mass hierarchy and CP phase, also requires much better understanding of resonant and coherent cross-sections. Precision measurement of nuclear effects and exclusive cross-sections will provide the necessary foundation for the study of neutrino oscillation with high-luminosity beams at the Fermilab Proton Driver whose unprecedented statistical power will otherwise be compromised by systematic uncertainties. It is essential to emphasize that the same careful study of cross-sections and nuclear effects must be performed with *antineutrinos* in order to understand mass effects and CP violation.

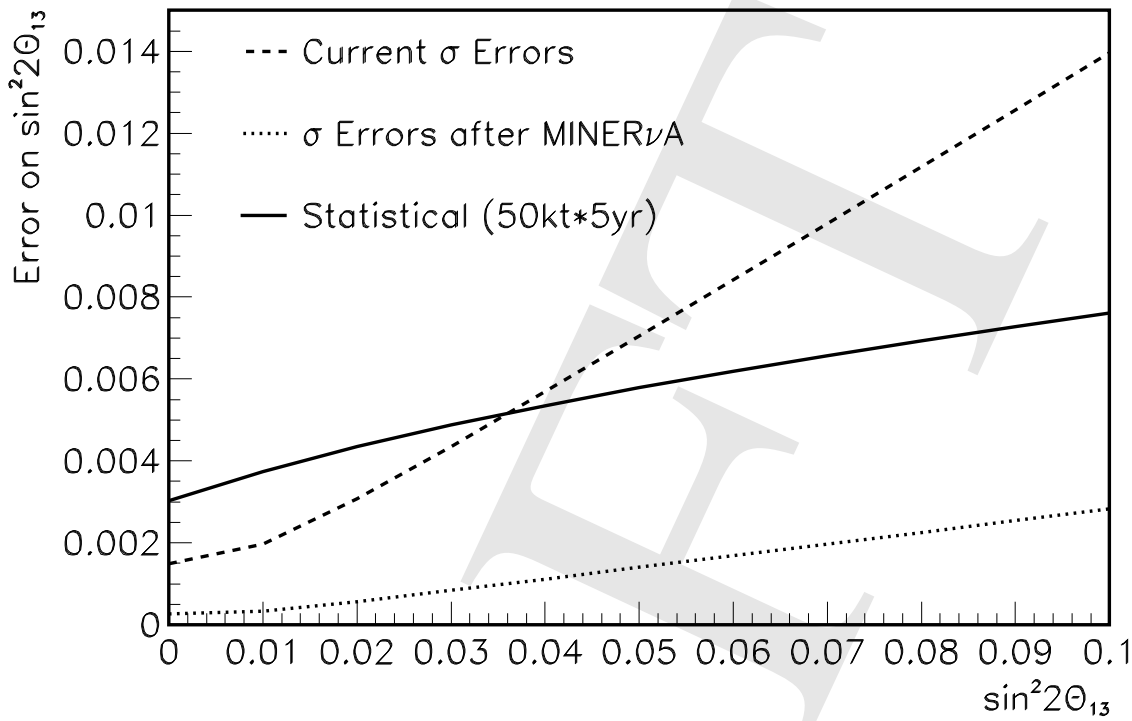

Figure 9: Statistical error, current cross-section systematic errors, and post-MINERνA cross-section systematic uncertainties in a NOνA measurement of $\sin^2 2\theta_{13}$, as a function of $\sin^2 2\theta_{13}$.

3.2 Neutrino Scattering Physics Program

Neutrino and antineutrino scattering measurements are of interest for a variety of reasons. Charged Current (CC) Quasi-Elastic (QE) scattering probes the structure of the nucleon and the binding of nucleons within the nucleus. Neutral Current (NC) elastic scattering probes the spin structure of the nucleon and the strange quark contribution. Resonant and coherent pion production probes the resonant structure of the nucleon and provides tests of non-perturbative QCD. Strange particle production measurements are needed to better understand backgrounds important in proton decay searches, and neutrino-electron elastic scattering can be used to search for physics beyond the Standard Model. In more detail:

(i) **Parton Distribution Functions** The neutrino structure functions F_1, F_2, and F_3 are given by:

$$F_2^{\nu,\bar{\nu}} = 2xF_1^{\nu,\bar{\nu}} = 2x\sum_q c_q^{\nu,\bar{\nu}} q(x,Q^2)$$

where $c_q^{\nu} = 1$ for $q = d, s, \bar{u}, \bar{c}$ and $c_q = 0$ for $q = u, c, \bar{d}, \bar{s}$ and vice versa for $\bar{\nu}$.

$$F_3^{\nu,\bar{\nu}} = 2\sum_q \tilde{c}_q^{\nu,\bar{\nu}} q(x,Q^2)$$

where $\tilde{c}_q^\nu = 1$ for $q = d, s$ and -1 for $q = \bar{u}, \bar{c}$, etc.

Precision measurements of structure functions using both neutrinos and antineutrinos allow determination of $q - \bar{q}$. Our knowledge of the the parton distributions is still very incomplete. For example, although we know that the net number of strange quarks is zero, there is no reason for $s(x) = \bar{s}(x)$. A global analysis to determine the strange sea asymmetry as a function of x shows moderate deviations from zero at higher Q^2. Differences between s and $\bar{s}$ can have a significant impact on the extraction of $\sin^2\theta_W$ from $\nu, \bar{\nu}$ data [96]. Even the valence PDFs are not well known at large x. The ratio of d/u is normally determined by comparing scattering from the proton and neutron. However, because no free neutron target exists, the deuteron is used as a neutron target. Although this makes little difference in the extracted value at small x, uncertainties in the nuclear corrections become substantial for x larger than about 0.6, and make determination of the ratio essentially impossible for x larger than about 0.8, as shown in Fig. 10. The ratio of d/u can be determined without any nuclear

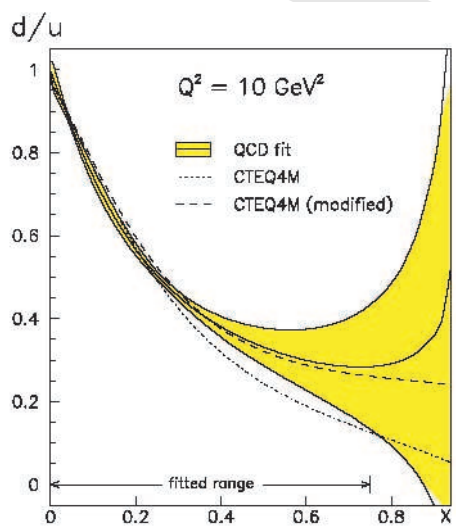

Figure 10: The d/u ratio showing the uncertainty due to nuclear effects in the deuteron. Figure taken from Ref. [97].

structure effect corrections by using neutrino and antineutrino scattering on hydrogen, as the ratio $F_2^{\nu p}/F_2^{\bar{\nu} p}$ is equal to d/u. Hence, a MW-scale Proton Driver would enable progress in obtaining a more complete knowledge of the parton distributions within the nucleon.

(ii) **Generalized Parton Distribution Functions** One of the most exciting developments of in the theory of the structure of the nucleon has been the understanding of generalized parton distributions (GPDs) [98–102]. The usual PDFs are sensitive only to the longitudinal momentum distributions of the parton. In contrast, the elastic form factors integrate over the longitudinal distributions of the partons and describe the spatial distribution. The GPDs give a more

complete picture of the nucleon in which the spatial distribution can be determined as a function of the longitudinal momentum distribution. However, the GPDs are difficult to access experimentally because they require measurement of exclusive final states. The most promising reaction to date is deeply virtual Compton scattering (DVCS), i.e. $p(e, e'\gamma p)$. These measurements are either underway or planned at JLab. However, a complete determination of the GPDs requires flavor separation which can only be accomplished using neutrinos and anti-neutrinos. Because of the requirement that exclusive final states be measured, the reaction is difficult to perform on nuclei. Although MINERνA will measure GPDs on carbon, due to nuclear effects this is considerably inferior to measurement on the proton. A true GPD measurement would require measurement of the $p(\bar{\nu}, \mu\gamma n)$ reaction using a free proton (i.e. hydrogen) target or $n(\nu, \mu\gamma p)$ reaction using a free neutron target (in practice, a deuteron target). Estimates for this "weak DVCS" process are currently being made by A. Psaker [103]. The CC cross section is of order 10^{-41}cm^2 and the NC about 10 times smaller. These small cross sections will clearly require higher intensity neutrino beams than are available at NuMI if measurements on hydrogen are to be performed.

(iii) **Strange Quarks and the Spin Structure of the Nucleon** The NC elastic scattering of neutrinos and antineutrinos on nucleons ($\nu N \to \nu N$, $\bar{\nu} N \to \bar{\nu} N$) provides information about the spin structure of the nucleon. In particular, these scattering processes are sensitive to the isoscalar spin structure that results from strange quark contributions. Determination of the strange quark contribution to the nucleon Δs has been a major component of the JLab program. Note that Δs, has been measured to be ≈ -0.1 in deep-inelastic scattering (DIS) polarized lepton experiments [104]. However, the procedure to extract Δs from DIS data is subject to model dependence and assumes SU(3) symmetry. A precise measurement of NC elastic scattering would provide a direct measurement of Δs that is insensitive to theoretical assumptions. The ideal measurement would be of the $(\nu p \to \nu p)/(\nu n \to \mu p)$ cross-section ratio on a deuterium target. The proposed FINeSSE experiment was designed to determine Δs by making an accurate measurement of this cross-section ratio using the Fermilab Booster neutrino beam and a carbon target (liquid scintillator). The ultimate goal in this program requires measuring NC elastic scattering with both neutrinos and antineutrinos, with a large event sample, on *nucleon* targets, which will require a MW-scale proton source to produce a narrow band neutrino beam of high intensity.

(iv) **Neutrino-Electron Elastic Scattering and the Neutrino Magnetic Moment** The Standard Model predictions for neutrino-electron elastic scattering have little theoretical uncertainty, and a measurement of $\nu e \to \nu e$ scattering can therefore be used in principle to precisely determine $\sin^2\theta_W$, and search for physics beyond the Standard Model. However, absolute cross-section measurements with the required precision are challenging, and may not be possible,

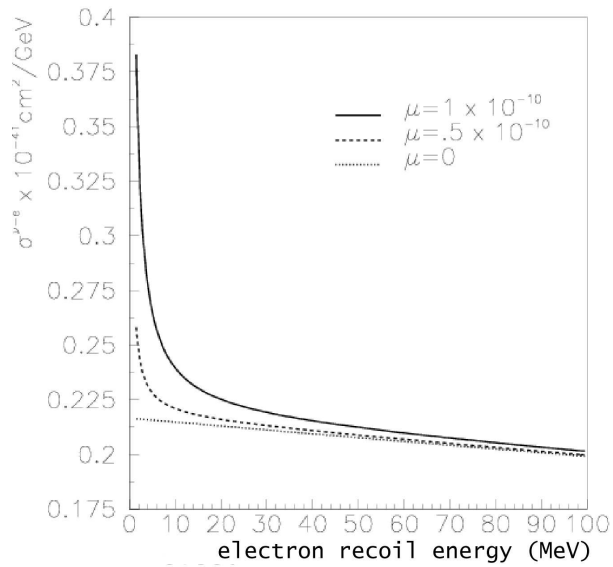

Figure 11: Differential cross section versus electron recoil kinetic energy, T, for $\nu e \to \nu e$ events. The electroweak contribution is linear in T (bottommost line), while contributions from nonzero neutrino magnetic moments yield sharp rises at low T.

even with a proton-driver class neutrino beam. An alternative strategy is to measure the well-predicted energy-dependent shape of the cross section. This would enable a search for physics beyond the Standard Model. As an example, consider a search for a finite neutrino magnetic moment, which is theoretically possible since we now know that neutrinos have finite masses. Within the Standard Model, modified to include finite neutrino masses, neutrinos may acquire a magnetic moment via radiative corrections. With $m_\nu = 1$ eV, the resulting magnetic moment would be $\approx 3 \times 10^{-19}\mu_B$ where $\mu_B = e/2m_e$ is the Bohr magneton. This value is too small to be detected or to affect astrophysical processes. Hence, a search for a finite neutrino magnetic moment is a search for physics beyond the Standard Model. The current best limit on the muon neutrino magnetic moment is $\mu_{\nu_\mu} \leq 6.8 \times 10^{-10}\mu_B$ from LSND $\nu_\mu e$ elastic scattering [105]. This sensitivity may be substantially improved, perhaps to the level of some beyond-the- Standard-Model predictions (which in some cases are as large as $10^{-11}\mu_B$), by precisely measuring the elastic scattering rate as a function of electron recoil energy. An electromagnetic contribution to the cross section from the magnetic moment will show up as an increase in event rate at low electron recoil energies (see Figure 11). The needed sensitivity requires a MW-class Proton Driver to produce a sufficiently intense neutrino beam, and a precise tracking detector with a low electron energy threshold. Depending on the energy threshold, a gain of 10-30 over the LSND measurement is possible.

(v) **Elastic Form Factors** The distributions of charge and magnetism within the

nucleus can be parameterized using two elastic form factors: the electric form factor G_E and the magnetic form factor G_M. For many years it was assumed that both the charge and magnetic distributions fall exponentially. With this assumption it can be shown that G_E and G_M are described by the "dipole" form. However, precision measurements at JLab [106, 107] have shown that this is not the case; the electric form factor has a distinctly different form, and drops more quickly than the magnetic form factor (Fig. 12), indicating that the charge distribution has a broader spatial distribution than the distribution of magnetism. In the language of particle physics, Perturbative QCD predicts that

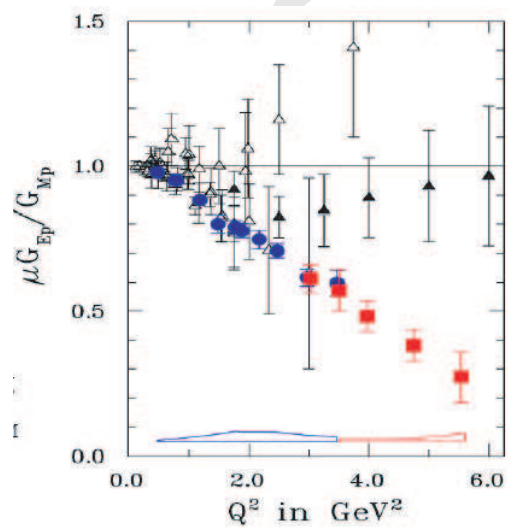

Figure 12: Ratio of the electric to magnetic form factor measured using polarization transfer. Data taken from Ref. [107].

the ratio Q^2F_1/F_2 should be constant. Instead it appears QF_1/F_2 approaches a constant. Although the reason for this is not understood, it does appear to be an indication of angular momentum between the quarks. To understand this more deeply it is desirable to precisely measure the weak form factor. This can be measured through parity violation in electron-nucleon scattering, with limited precision. Neutrino-nucleon elastic (or quasi-elastic) scattering depends on both the electromagnetic form factors and the weak form factor. Nearly half the cross section is due to the weak form factor, making neutrino-nucleon scattering a good probe. Proposed measurements of the weak form factor (e.g. the MINERνA experiment) use scattering from nucleons in nuclei. Although the statistical precision will be reasonably good, there is an uncertainty in both extracting the form factor from scattering from a bound nucleon due to final state interactions and other conventional effects, as well as the possibility of modification of the form factor by the nuclear medium. Thus, measurement of the form factor using neutrino scattering on hydrogen and deuterium is essential. This will require the intensity available at a MW-scale Proton Driver.

(vi) **Duality and Resonance Production** Although QCD appears to provide a

good description of the strong interaction, we have a very poor understanding of the transition from the domain where quarks and gluons are the appropriate degrees of freedom to the domain best described using baryons and mesons. In the region of modest Q^2 (1-10 GeV^2) the scattering of electrons on nucleons is dominated by resonance production, and can also be described using the same formalism as DIS. However, there is no obvious reason to expect the structure functions measured in the resonance region from correlated partons forming the nucleon should be related to the DIS structure functions. Despite this, experiments at JLab [108] have found that the F_2 structure function measured in the resonance region closely follows that measured in the DIS region. The phenomenon, called quark-hadron duality, has also been observed in other processes, such as e^+e- annihilation into hadrons. The origins of duality are not well understood [109–116]. It is expected that duality should also exist for weak interactions, however the present data are not of sufficient quality to provide a clean test of this. The next decade of experiments, especially with MINERνA, should provide some information on the validity of duality using neutrinos. However, high precision measurements using anti-neutrinos and nucleon (hydrogen and deuterium) targets will be required in order to fully explore the origins of duality.

(vii) **Strange Particle Production** Measurements of the production of strange mesons and hyperons in neutrino NC and CC processes (e.g. $\nu_\mu n \to \mu^- K^+ \Lambda^0$ and $\nu_\mu p \to \nu_\mu K^+ \Lambda^0$) provide input to test the theoretical models of neutrino induced strangeness production [117, 118]. In addition, neutrino induced strangeness production is a significant background in searches for proton decay based on the SUSY-inspired proton decay mode $p \to \nu \Lambda K^+$. The existing experimental data on these channels consists of only a handful of events from bubble chamber experiments. There are plans to measure these reactions using the existing K2K data and the future MINERνA data. MINERνA will collect a large sample ($\approx 10,000$) of $\nu_\mu n \to \mu^- K^+ \Lambda^0$ events. However, the antineutrino measurements will require a more intense (MW-scale) proton source.

3.3 The Need for a High Intensity Proton Beam at 8 GeV

The Fermilab long-baseline neutrino oscillation program utilizes the NUMI beamline, and hence protons at MI energies. It is important to stress that the desired neutrino scattering program at a MW-class proton driver would utilize both the upgraded MI beam and the high-intensity lower energy proton beam at 8 GeV. The measurements using high-intensity neutrino and antineutrino beams of mean energy ≈ 1 GeV are particularly important. These measurements require that the beam have no high-energy tail (above ≈ 2 GeV) so that backgrounds from multipion and deep-inelastic scattering processes do not overwhelm the signal reactions of interest. The energy distribution of the booster neutrino beam, currently in operation at Fermilab, is ideal for these studies (Fig. 13). An 8 GeV MW-class proton-driver beam that uses a MiniBooNE-like horn-focusing system would satisfy the beam requirements. A

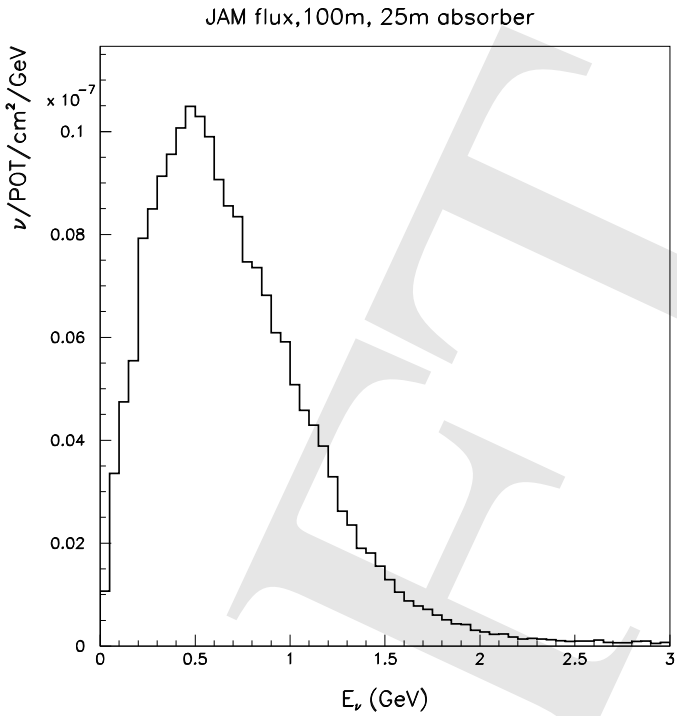

Figure 13: Calculated ν_μ flux at a 100m location on the booster neutrino beamline.

2 MW beam at 8 GeV would enable a 64-fold increase in intensity with respect to MiniBooNE. This is the rough factor required to enable precision neutrino and antineutrino measurements using nucleon targets. In addition to the highest intensities practical, it is also important for the neutrino beam to have a very low duty-factor. This will require a buncher using either the recycler ring or a new dedicated storage ring. Note that beam-unrelated cosmic-ray-induced backgrounds increase with the duty-factor. Many of the desired neutrino measurements require low backgrounds for low energy final states (e.g. NC elastic scattering and neutrino-electron elastic scattering). These measurements would be limited with a high duty-factor neutrino beam.

4 The Broader Proton Driver Physics Program

In the past high precision measurements at low energies have complemented the experimental program at the energy frontier. These low energy experiments not only probe mass scales that are often beyond the reach of colliders, but also provide complementary information at mass scales within reach of the energy frontier experiments. Examples of low energy experiments that have played an important role in this way are muon g-2 measurements, searches for muon and kaon decays beyond those predicted by the Standard Model, measurements of rare kaon processes, etc. A summary of the sensitivity achieved by a selection of these experiments is given in Fig. 14. It seems likely that these types of experiment will continue to have a critical role as the energy frontier moves into the LHC era. In particular, if the LHC discovers new

DRAFT

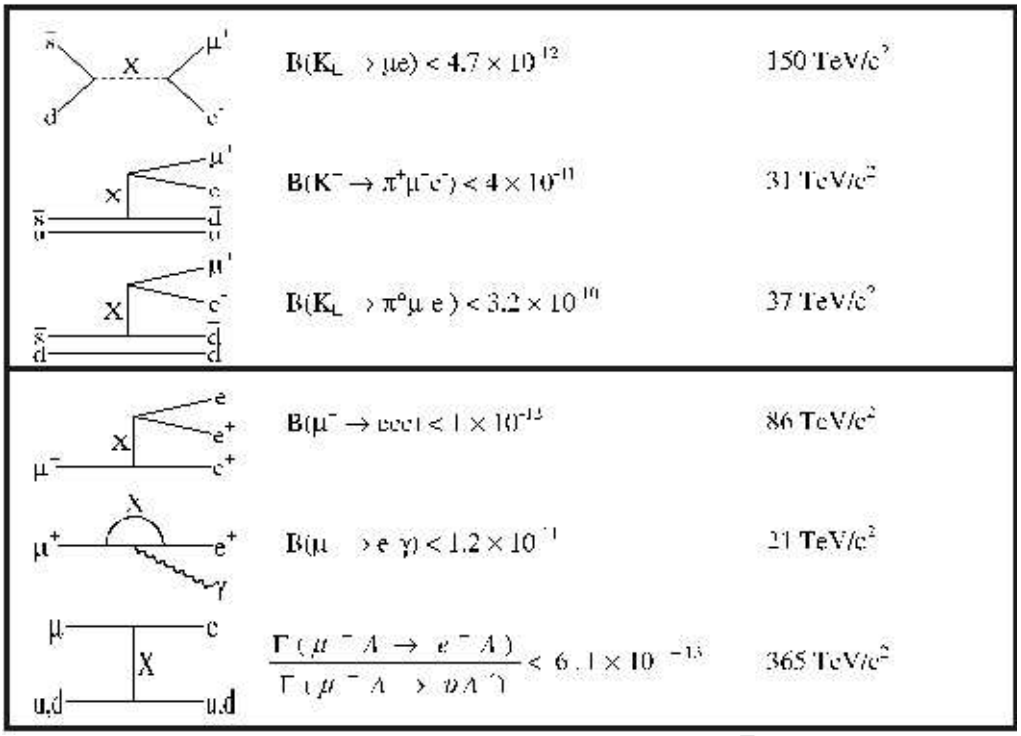

Figure 14: Current limit on Lepton Flavor Violating processes and the mass scales probed by each process. The upper box is for kaon decays, which involve a change of both quark flavor and lepton flavor. The bottom box is for muon decays, which involve only lepton flavor change. The lower limit on the mass scale is calculated assuming the electroweak coupling strength.

physics beyond the Standard Model, the measurement of quantum corrections that manifest themselves in low energy experiments would be expected to help elucidate the nature of the new physics. If no new physics is discovered at the LHC then precision low energy experiments may provide the only practical way of advancing the energy frontier beyond the LHC in the foreseeable future.

4.1 Muon Physics

Solar-, atmospheric-, and reactor-neutrino experiments have established Lepton Flavor Violation (LFV) in the neutrino sector, which suggests the existence of LFV processes at high mass scales. Depending on its nature, this new physics might also

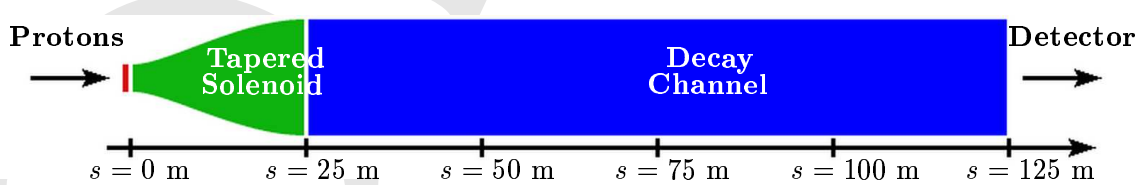

Figure 15: Schematic of the solenoid-based muon source discussed in the text. This performance of this channel has been simulated using the MARS code.

produce observable effects in rare muon processes. Furthermore, CP Violation in the charged lepton sector, revealed for example by the observation of a finite muon Electric Dipole Moment (EDM), might be part of a broader Baryogenesis via Leptogenesis picture. Hence, the neutrino oscillation discovery enhances the motivation for a continuing program of precision muon experiments. In addition, the expectation that there is new physics at the TeV scale also motivates a new round of precision muon experiments. LFV muon decays and the muon anomalous magnetic moment $a_\mu = (g-2)/2$ and EDM are sensitive probes of new dynamics at the TeV scale. In general, with sufficient sensitivity, these experiments would help elucidate the nature of new physics observed at the CERN Large Hadron Collider (LHC). As an example, in SUSY models the muon (g-2) and EDM are sensitive to the diagonal elements of the slepton mixing matrix, while LFV decays are sensitive to the off-diagonal elements. If SUSY is observed at the LHC these precision muon experiments would provide one of the cleanest measurements of $\tan\beta$ and of the new CP Violating phases. It is possible that no new physics will be observed at the LHC. In this case precision muon experiments might provide, for the foreseeable future, one of the few practical ways to probe physics at higher mass scales. Note that the Brookhaven (g-2) Collaboration have reported a value for (g-2) that is 2.7 standard deviations away from the Standard Model prediction. Noting that the muon (g-2) is sensitive to any new heavy particles that couple to the muon, it is possible that the current measurements are providing an early indication of the existence of new TeV-scale particles. Higher precision measurements are well motivated.

4.1.1 The Muon Source

Low energy high precision muon experiments require both high intensity beams and a bunch structure that is appropriate for the experiment. Hence two ingredients needed to produce an "ideal muon source" are (i) a high intensity proton source, and (ii) a way of producing the desired bunch structure. Since different muon experiments require different bunch structures the ideal source would also be sufficiently flexible to provide different bunch structures. With an upgraded Proton Driver Fermilab would have the desired high intensity proton source. In addition, in the post-collider period it might be possible to utilize the Recycler Ring to repackage the 8 GeV proton beam, yielding the desired bunch structure. The combination of Proton Driver plus Recycler Ring would provide the front-end for a unique muon source with intensity and flexibility that exceed any existing facility.

The Recycler is an 8 GeV storage ring in the MI tunnel that can run at the same time as the MI. The Recycler is currently used for antiproton production for the Fermilab collider program. The beam from the proposed Proton Driver linac that is not used to fill the MI could be used to fill the Recycler Ring approximately ten times per second. The ring could then be emptied gradually in the 100 ms intervals between linac pulses. Extraction could be continuous or in bursts. For example, the Recycler Ring could be loaded with one linac pulse of 1.5×10^{14} protons every 100 ms, with one missing pulse every 1.5 seconds for the 120 GeV MI program. This provides $\sim 1.4 \times 10^{22}$ protons at 8 GeV per operational year (10^7 seconds). In the Recycler

Experiment		I_0/I_m	δT [ns]	ΔT [μs]	p_μ [MeV]	$\Delta p_\mu/p_\mu$ [%]
$\mu A \to eA$	10^{21}	$< 10^{-10}$	< 100	> 1	< 80	< 5
$\mu \to e\gamma$	10^{17}	n/a	n/a	n/a	< 30	< 10
$\mu \to eee$	10^{17}	n/a	n/a	n/a	< 30	< 10
$\mu e \to \mu e$	10^{16}	$< 10^{-4}$	< 1000	> 20	< 30	1...2
τ_μ	10^{14}	$< 10^{-4}$	100	> 20	30	< 10
g_μ-2	10^{15}	$< 10^{-7}$	< 50	$> 10^3$	3100	< 2
EDM	10^{16}	$< 10^{-6}$	< 50	$> 10^3$	<1000	< 2

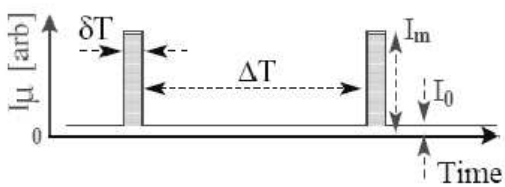

Figure 16: Beam requirements for new muon experiments. Given are the minimum total number of muons above which significant progress can be made, the muon suppression between pulses, the length and separation of pulses and the momentum spread of the muon beam.

each pulse of 1.5×10^{14} protons can be chopped into 588 bunches of 0.25×10^{12} protons/bunch with a pulse width of 3 ns. A fast kicker allows for the extraction of one bunch at a time. The beam structure made possible by the proton driver linac and the Recycler Ring is perfect for $\mu \to$ e conversion experiments, muon EDM searches and other muon experiments where a pulsed beam is required. Slow extraction from the Recycler Ring for $\mu \to e\gamma$ and $\mu \to 3e$ searches is also possible.

The performance of the strawman muon source shown in Fig. 15 has been simulated using the MARS code. The evolution of the pion and muon spectra down the decay channel is shown in Fig. 17 and the calculated fluxes are summarized in Table 5. The scheme will yield ~ 0.2 muons of each sign per incident 8 GeV proton. With 1.4×10^{22} protons at 8 GeV per operational year this would yield $\sim 3 \times 10^{21}$ muons per year. This muon flux greatly exceeds the flux required to make progress in broad range of muon experiments (see Fig 16). However, the muons at the end of the decay channel have a large momentum spread and occupy a large transverse phase space. Without further manipulation their utilization will be very inefficient. The additional beam manipulating interface between the decay channel and each candidate experiment has yet to be designed. In Japan a Phase Rotated Intense Slow Muon Source (PRISM) based on an FFAG ring that reduces the muon energy spread (phase rotates) is being designed. This phase rotation ring has a very large transverse acceptance (800π mm-mrad) and a momentum acceptance of $\pm 30\%$ centered

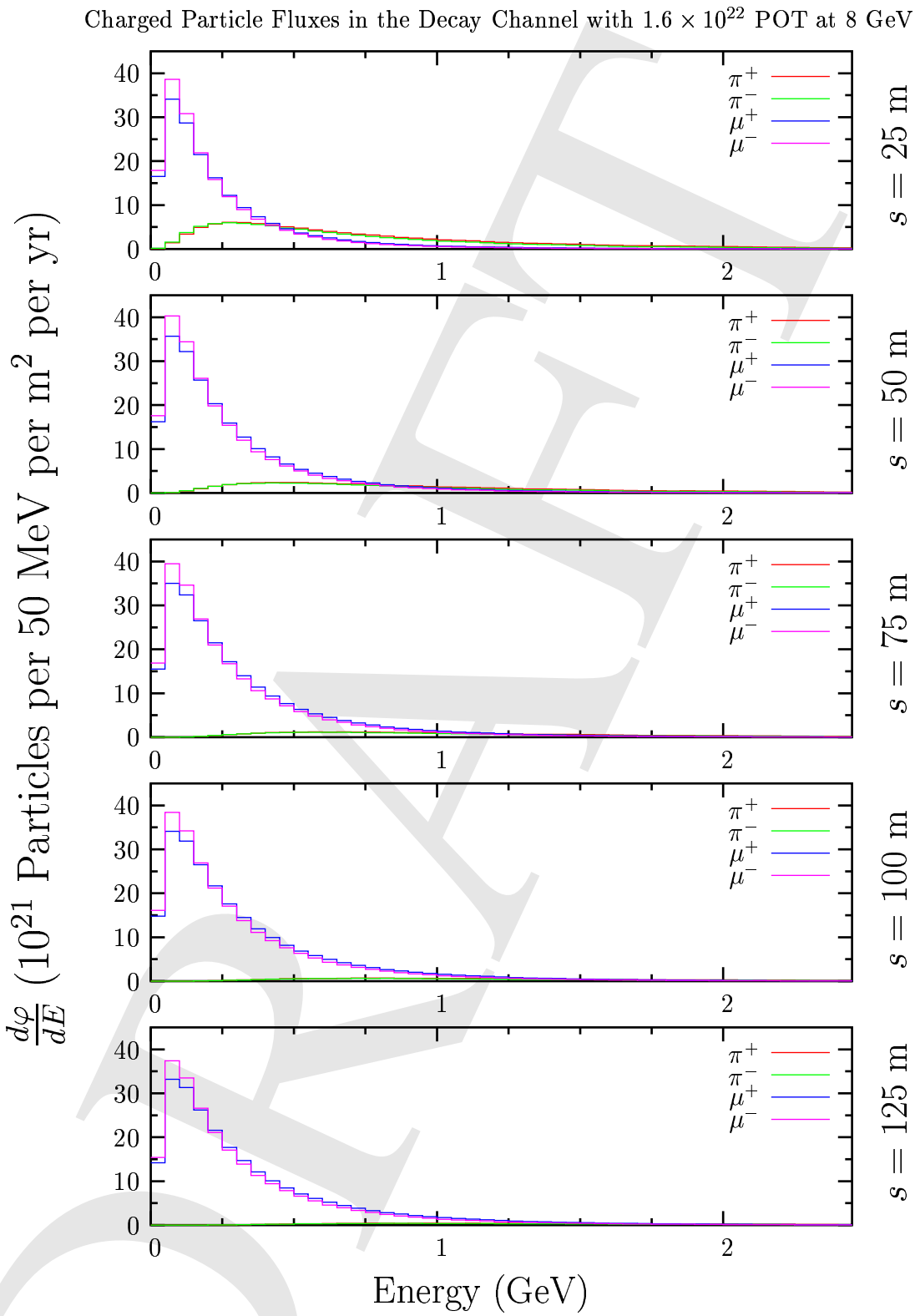

Figure 17: Charged particle fluxes at various positions down the 100 m decay channel with a 30 cm beampipe radius. The normalization corresponds to an 8 GeV, 2 MW proton driver in operation for a 10^7-s year.

DRAFT

at 500 MeV/c. PRISM reduces the momentum and momentum spread to 68 MeV/c and $\pm 1 - 2\%$ respectively. Hence, a PRISM-like ring downstream of the decay channel might accept a significant fraction of the muon spectrum (Fig. 17) and provide a relatively efficient way to use the available muon flux. Explicit design work must be done to verify this, but it should be noted that a muon selection system that utilizes only 1% of the muons available at the end of the decay channel will still produce an adequate muon flux for most of the cutting-edge experiments described in the following sections.

Finally, a new 8 GeV multi-MW Proton Driver at Fermilab, together with an appropriate target, pion capture and decay channel, would not only provide a new World Class facility for low energy muon experiments, but could also provide the first step toward a Neutrino Factory based on a muon storage ring. In the initial phase the muon beam produced in the pion decay channel would occupy a relatively large phase space. The first generation of muon experiments would use only those muons within a small part of this phase space. This muon source could then be upgraded in one or more steps with the addition of phase rotation (if not already included in the initial muon source) and cooling channels to produce a cold muon beam occupying a phase space that fits within the acceptance of an accelerator (perhaps the Proton Driver Linac). At this point the number of useful muons available for low energy muon experiments will be greatly increased. In addition, new experiments using medium energy beams of a few GeV will also become possible. Finally, the acceleration scheme would be upgraded to produce muon beams of 20 GeV or more and a muon storage ring constructed with long straight sections pointing in the desired direction. This last step would realize a Neutrino Factory, perhaps sometime within the next two decades, or on a longer timescale if a Linear Collider is constructed near Fermilab.

4.1.2 Electric Dipole Moment

Electric Dipole Moments violate both parity (P) and time reversal (T) invariance. If CPT conservation is assumed, a finite EDM provides unambiguous evidence for CP violation. In the Standard Model EDMs are generated only at the multi-loop level,

	$s = 25$ m	$s = 50$ m	$s = 75$ m	$s = 100$ m	$s = 125$ m
μ^+/P	0.16	0.20	0.21	0.21	0.22
μ^-/P	0.16	0.20	0.21	0.21	0.21
π^+/P	0.095	0.051	0.030	0.020	0.014
π^-/P	0.087	0.044	0.025	0.016	0.011

Table 5: The number of charged particles in the beam per incident 8 GeV primary proton as a function of the distance downstream from the target. These numbers are computed using the MARS code. The normalization corresponds to a 2 MW proton driver.

and are predicted to be many orders of magnitude below the sensitivity of foreseeable experiments. Observation of a finite muon EDM (d_μ) would therefore provide evidence for new CP Violating physics beyond the Standard Model. CP violation is an essential ingredient of almost all attempts to explain the matter-antimatter asymmetry of the Universe. However, the measured CP Violation in the quark sector is known to be insufficient to explain the observed matter-antimatter asymmetry. Searches for new sources of CP violation are therefore well motivated.

A number of extensions to the Standard Model predict new sources of CP violation. As an example, in SUSY models in which finite neutrino masses and large neutrino mixings arise from the seesaw mechanism, d_μ can be significant. If the seesaw mechanism is embedded within a left-right symmetric gauge structure the interactions responsible for the masses of right-handed Majorana neutrinos can produce values of d_μ as large as 5×10^{-23} e-cm. This is well below the present limit $d_\mu < 3.7\times10^{-19}$ e-cm, but would be within reach of a new dedicated experiment at a high intensity muon source. The muon EDM group has proposed an experiment at JPARC to obtain a sensitivity of 10^{-24} e-cm. This sensitivity would still be limited by statistics. Higher muon intensities would help, although the measurement would also be rate limited. To obtain a sensitivity of O(10^{-26}) e-cm would require an improved beam structure with many short pulses, each separated by at least 500 μs. Hence, depending on the fate of the JPARC proposal, a muon EDM experiment at a Fermilab Proton Driver would be designed to obtain a sensitivity somewhere in the 10^{-24} - 10^{-26} e-cm range.

4.1.3 Muon g-2

The Brookhaven (g-2) Collaboration has reported a value that is 2.7 standard deviations from the Standard Model prediction. This could be an early indication of new physics at the electroweak symmetry breaking scale. Physics that would affect the value of (g-2) include muon substructure, anomalous gauge couplings, leptoquarks, and SUSY. In particular, in a minimal supersymmetric model with degenerate sparticle masses the contribution to the anomalous magnetic moment a_μ could be substantial, particularly for large $\tan\beta$. To illustrate the possibilities it is useful to consider the large $\tan\beta$ approximation with degenerate SUSY masses. The estimated range of SUSY masses that correspond to the observed a_μ are 100 - 450 GeV for $\tan\beta = 4-40$. Hence the present (g-2) experiment is probing the mass range of interest for electroweak symmetry breaking. Within the next few years, with further data taking the BNL experiment might be able to improve sensitivity by a factor of a few. To make progress beyond this will require either an upgraded storage ring or a new ring, and a higher intensity muon source. A high intensity muon source at a Fermilab Proton Driver would provide a natural home for this next generation experiment.

The current measurement of $a_\mu = (g-2)/2$ is accurate to 0.46 (stat) $\pm$ 0.27 (sys) ppm. An proposed upgrade to the current program could reduce the systematic error by a factor of 2 and increase the statistical sample by a factor of 9. This would increase the overall precision from 0.5 ppm to 0.2 ppm. Combined with expected near-term improvements in theory, this could lead to a significant confrontation with the Standard Model. A new, dedicated g$-$2 experiment could improve the overall

precision by a factor of 10. This could be accomplished by reducing the systematic error by a factor of 7 and increasing the statistical sample by a factor of 200. A long list of improvements necessary to reduce the systematic error has been identified by the g-2 group. These include use of a backward muon beam, a longer pion decay beamline and better phase space matching of the beamline to the ring. Particle pile-up will ultimately limit the sensitivity of future searches. To reduce pile-up, a pulsed beam (<20 ns) with a high repetition rate and a minimum of 1 ms between pulses would be most advantageous.

4.1.4 Rare Muon Decays

If a negative muon is stopped in a target it will be captured by an atom and then cascade down to the $1s$ state. In the Standard Model the muon will either decay in orbit or will be captured by the nucleus with the emission of a neutrino. In LFV models beyond the Standard Model the muon can also be converted into an electron in the field of the nucleus ($\mu \to e$ conversion) or can undergo non-Standard Model decays ($\mu \to e\gamma$, $\mu \to eee$, ...). In the Standard Model, extended to include the seesaw mechanism with right-handed neutrinos in the mass range 10^{12} to 10^{15} GeV, the predicted LFV decay branching ratios are unobservably small. However in SUSY seesaw models, parametrized at the GUT scale by the right-handed Majorana mass matrix and the neutrino Yukawa matrix, the Yukawa couplings induce off-diagonal mixing matrix elements at the one-loop level. The resulting LFV decay branching ratios can be significant. The predicted branching ratios depend upon the origin of SUSY breaking. Muon LFV decay searches therefore place constraints on SUSY breaking schemes.

Consider first $\mu \to e\gamma$. The present limit on the decay branching ratio is 1.2×10^{-11}. Within the context of SUSY models, this limit already constrains the viable region of parameter space. The MEG experiment at PSI is expected to reach a branching ratio sensitivity of 10^{-14} by the end of the decade. The MEG measurement will provide constraints on SUSY parameter space complementary to those obtained by the LHC experiments. If MEG observes $\mu \to e\gamma$ then both a higher statistics experiment and new searches for other non-Standard Model decay modes will be well motivated. If MEG only obtains a limit, further progress will also require a more sensitive experiment. In either case, a $\mu \to e\gamma$ experiment at a new Fermilab Proton Driver would provide a way forward provided a high sensitivity experiment can be designed to exploit higher stopped muon rates. Progress will depend upon improvements in technology to yield improved background rejection and higher rate capability. Background rejection depends upon track pointing resolution, energy resolution, and timing resolution. Fortunately, we can anticipate significant improvements in tracking technology in the next few years, and corresponding improvements in the critical detector resolutions and rate capability. To illustrate the possible gains in the $\mu \to e\gamma$ sensitivity consider an experiment that uses pixel detectors to track both the decay positron and the electron-positron pair from the converted photon. It has been shown that if BTeV pixel technology is used in an idealized geometry (Fig. 18), but with only 10% of the coverage of the old MEGA experiment, then a sensitivity that

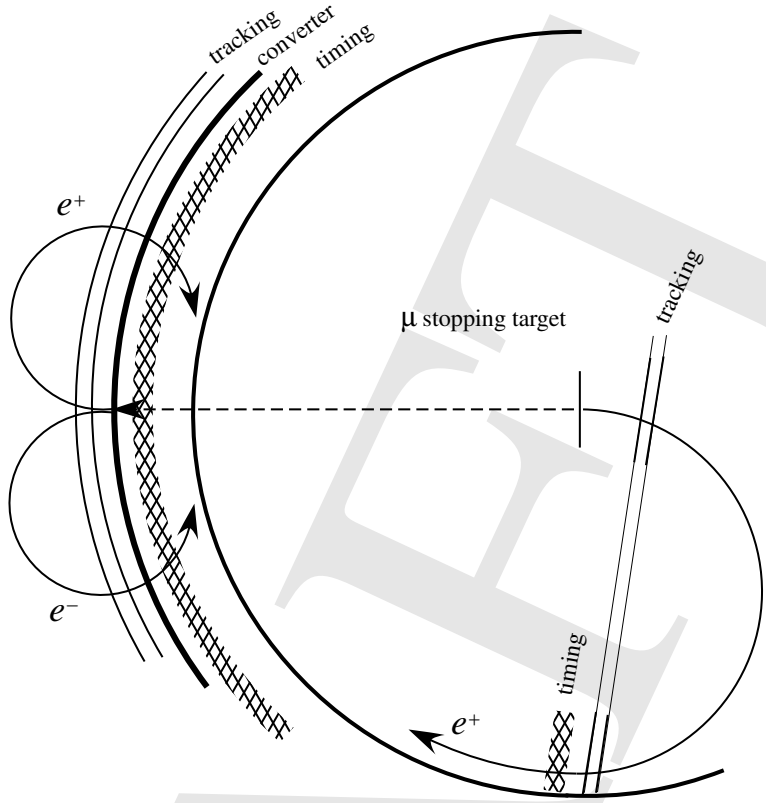

Figure 18: Fritzs egamma detector

is comparable to the expected MEG sensitivity might be obtained at a beamline of the sort to be used by the BNL MECO experiment. Hence, pixel technology already offers an alternative to the traditional low mass tracking technology used in $\mu \to e\gamma$ experiments. The main limitation in using BTeV pixel technology would come from scattering in the fairly thick detectors. We can anticipate the development of much thinner pixel detectors. If, in the coming years, the pixel thickness can be reduced by a factor of 10, coverage increased to 50% of the MEGA coverage, and the readout rate improved by a factor of 20, then the resulting single event sensitivity would be improved by about two orders of magnitude. With even higher rate pixel detectors a further order of magnitude improvement might be possible.

Now consider $\mu \to e$ conversion. Within the context of SUSY extensions to the Standard Model, the $\mu \to e$ conversion rate is related to the $\mu \to e\gamma$ branching ratio:

$$\Gamma(\mu \to e\gamma) \sim 16\alpha^4 Z_{eff}^4 Z |F(q^2)|^2 BR(\mu \to e\gamma) \tag{4}$$

where Z is the proton number for the target nucleus, Z_{eff} is the effective charge, and $F(q^2)$ is the nuclear form factor. The $\mu \to e$ conversion rate normalized to the muon capture rate in Ti is then given by:

$$R(\mu^- \to e^- \, Ti) \sim 6 \times 10^{-3} BR(\mu \to e\gamma) \tag{5}$$

The prediction is model dependent, and hence searches for both $\mu \to e\gamma$ and $\mu \to e$ conversion are well motivated. The apparent suppression of the $\mu \to e$ conversion

rate with respect to the $\mu \to e\gamma$ decay rate is in practice compensated by the higher sensitivity achievable for the conversion experiments. At BNL the MECO experiment is expected to achieve a sensitivity of O(10^{-17}) in the coming decade. In the longer term the PRIME experiment has been proposed at JPARC to improve the sensitivity to O(10^{-19}). Proton economics may well determine the fate of PRIME. If PRIME is not able to proceed at JPARC it might be accommodated at a Fermilab Proton Driver. If PRIME does proceed in Japan, a further generation experiment might be justified, but its design would presumably need to benefit from lessons learned with MECO and PRIME.

4.1.5 Other Muon Experiments

High precision future muon EDM, (g-2), and rare decay experiments, together with the possible development of a Neutrino Factory, provide the main particle physics motivation for desiring a new low energy high intensity muon source. There are however other measurements that might further enrich the scientific program at a new muon source, and provide an opportunity for smaller scale experiments. Muonium studies and precision muon lifetime measurements are examples of these types of experiment. Muonium experiments provide precision tests of QCD, precision measurements of the fine structure constant, m_μ/m_e, the structure of the proton, and of course a search for lepton flavor violation. Many of these measurements are statistics limited. Higher precision muon lifetime measurements would provide a more precise value of the Fermi constant G_F. The theoretical uncertainty in the extraction of G_F is < 0.3 ppm. At PSI the MuLAN experiment as attempting to measure G_F with a precision of 1 ppm. A second PSI experiment, MuCAP, is measuring the muon capture rate to extract the pseudoscalar form factor g_p with a precision of 7%. Further progress on measuring G_F and g_p will require high intensity muon beams with small spot sizes and tiny energy spreads. Hence, a muon source at a new Fermilab Proton Driver might provide a home for a further generation of these experiments.

4.2 Kaons

The most important kaon decays to be studied in the future appear to be the ultra-rare FCNC modes $K^+ \to \pi^+\nu\nu$ and $K_L \to \pi^0\nu\nu$. The SM expectations for the associated branching ratios are at the $3 - 7 \times 10^{-11}$ level. These so-called "golden modes" are of interest since they can be predicted in the SM with high theoretical accuracy, and are sensitive to a wide variety of new physics beyond the Standard Model. For example, within the context of Minimal Flavor Violation models, an agreement of BR($K_L \to \pi^0\nu\nu$) with the SM prediction at the 1% level would constrain the new physics scale to exceed 12 TeV. The golden modes provide a search for new TeV-scale physics that is complementary to searches at the LHC, and could help elucidate the nature of any new states observed at the energy frontier and their associated couplings. The world sample of $K^+ \to \pi^+\nu\nu$ consists of 3 candidate events observed by the combined BNL-E787 and BNL-E949 experiments. The experimental central value for the branching ratio is $1.5^{1.3}_{-0.9} \times 10^{-10}$, consistent with the SM expectation. There are currently no

observed candidates for $K_L \to \pi^0\nu\nu$. A new generation of experiments has been proposed to observe 50-100 of each of these decay modes within the next 10 years. In the K_L sector, the initiatives are KOPIO at BNL, and KEK391a and the follow-up experiment at JPARC (LOI-05). In the K^+ sector, the initiatives are JPARC-LOI-04, NA48/3 at CERN, and P940 at Fermilab. These will be exceedingly difficult experiments. Since they are searching for 3-body decays, and the neutrinos are not detected, there will be no mass peak, and high instantaneous rates from backgrounds that can exceed the signal by 10 orders of magnitude must be tolerated. A long spill length and debunched beam are necessary. In the proton driver era, assuming the presently proposed experiments meet their 50-100 event goal, a reasonable next goal would be to carry out measurements at the 1000 event level. However, the near term experiments are already pushing the limit of detector technology. Progress will therefore require improvements in detector technology. Nevertheless, there are reasons to hope that the required improvements will be made. Assuming this is the case we can estimate the required number of protons on target. We consider a KAMI-like beam line and detector for the $K_L \to \pi^0\nu\nu$ case, and use efficiency numbers from the KAMI proposal. For the $K^+ \to \pi^+\nu\nu$ case, we extrapolate similar quantities from the P940 proposal. The required numbers of protons on target are given in Table 6.

Mode	Sample Size	Physics Measurement	POT
$K^+ \to \pi^+\nu\nu$	1000	3% of $\|V_{ts} * V_{td}\|$	$1.5 \cdot 10^{20}$
$K_L \to \pi^0\nu\nu$	1000	1.5% of $Im(V_{ts} * V_{td})$	$1.6 \cdot 10^{21}$
$K_L \to \pi^0 e^+ e^-$	$2 \cdot 10^4$	10% of $Im(V_{ts} * V_{td})$	$2.5 \cdot 10^{20}$
$K_S - K_L \to \pi^0 e^+ e^-$	10^5	10% of $Im(V_{ts} * V_{td})$	$2.4 \cdot 10^{23}$
$K_S - K_L \to \pi^0 e^+ e^-$	$4 \cdot 10^5$	10% of $Im(V_{ts} * V_{td})$	$2.5 \cdot 10^{23}$

Table 6: Desired data sample sizes for various kaon physics measurements in the Proton Driver era, and the associated number of protons on target (POT) needed.

Recently two additional decay modes have received attention: $K_L \to \pi^0 ee$ and $K_L \to \pi^0\mu\mu$. These decay modes are fully reconstructable, and therefore are significantly easier to identity than $K \to \pi\nu\nu$. There are no large backgrounds that could "feed-down" and fake the signal. The only serious backgrounds are $K_L \to ee\gamma\gamma$ and $\mu\mu\gamma\gamma$ which occur with a branching ratio of about 10^{-7} and can be reduced by kinematic cuts to obtain an effective residual background level of $\sim 10^{-10}$. Although this exceeds the expected signal by an order of magnitude, the background is flat over the signal region and with sufficient statistics the signal peaks would enable extraction of the branching ratios. The required numbers of protons on target are summarized in Table 6.

4.3 Pions

Pion experiments can provide precision tests of the Standard Model, searches for physics beyond the Standard Model, and measurements of light meson and baryon

states that help us to develop a better understanding of the confinement and symmetry properties of QCD. In more detail:

(i) **Pion Decays** Pions are the lightest hadrons. Their decay modes are few and simple, and they therefore provide an exquisite laboratory for testing fundamental symmetries. It is generally agreed that the next important step in pion decay physics is to accurately measure the branching ratio of the decay $\pi^+ \rightarrow e^+\nu(\gamma)$ (π_{e2}) and normalize it to $\pi^+ \rightarrow \mu^+\nu(\gamma)$ ($\pi_{\mu 2}$). The double ratio BR(π_{e2})/BR($\pi_{\mu 2}$) is theoretically clean, probes e-μ universality in weak charged decays, and is predicted in the Standard Model to have a value of $(1.2356 \pm 0.0001) \times 10^{-4}$. Beyond-the-SM scenarios typically preserve lepton universality in weak charged decays, and so it is believed to be a deeply fundamental symmetry. The current PDG2004 world average of the double ratio is $(1.230 \pm 0.004) \times 10^{-4}$. In comparison with lepton universality tests in τ-decays or W-decays, the pion system's experimental precision is $3 - 10\times$ better and is unlikely to be surpassed. Increasing the precision of the pion measurements would be extremely valuable, as the theoretical prediction is currently 40 times more precise. In addition, the π_{e2} measurement provides the normalization for measurements of the decay $\pi^+ \rightarrow e^+ n\pi^0$ decays (π_β). The uncertainty on the π_{e2} measurements dominate the external systematic uncertainties on the π_β measurement. This is of interest because the CKM matrix element V_{ud} can be extracted cleanly from π_β measurements. The current best π_β measurement yields $V_{ud} = 0.9728(30)$. The PDG average is $V_{ud} = 0.9738(5)$, which is dominated by measurements from super-allowed nuclear decays. However, in the future, improved π_β measurements would allow a theoretically cleaner extraction of V_{ud}, and improved precision provided the statistical and systematic uncertainties can be decreased. Finally, other rare pion decay modes that provide opportunities for searches for new physics are $\pi^0 \rightarrow 3\gamma$ for which the present best limit is $BR < 3.1 \times 10^{-8}$, $\pi^0 \rightarrow 4\gamma$ for which the present best limit is $BR < 2 \times 10^{-8}$, and $\pi^0 \rightarrow \nu\nu$ for which the present best limit is $BR < 8.3 \times 10^{-7}$. The PIBETA experiment at PSI is the current state-of-the-art charged pion decay experiment. PIBETA uses stopped pions. Neutral pion decays are studied using the charge-exchange reaction $\pi^- p \rightarrow \pi^0 n$. It is believed that the decay-at-rest technique is now at its systematic limit. At a Proton Driver, progress could be made by using decay-in-flight techniques. The main challenge would be to build an apparatus with reasonably large acceptance and, for the precision π_{e2} measurement, understand the acceptance at the 10^{-3} level. The advantages that make the decay-in-flight technique worth pursuing are that (a) there would be no target-degrader material which greatly reduces the beam interaction background, (b) there would be no rate limitation due to the the 2 μ sec length of $\pi - \mu - e$ decay chain at rest and the higher energy decay products would allow a more efficient rejection of backgrounds arising from the $\pi - \mu - e$ decay chain, (c) the normalization of the pion flux could be measured absolutely by a device such as a beam Cerenkov detector, and (d) a decay-in-flight experiment could also measure π^- decays. Hence, a Proton Driver could enable progress to be made

beyond PIBETA.

(ii) **Meson and Baryon Spectroscopy**

Light meson and baryon spectroscopy probes the confinement and symmetry properties of QCD. Beyond the usual meson and baryon states, QCD predicts exotic bound configurations of quarks and gluons which include hybrids (e.g. $q\overline{q}g$ and q^3g), pure gluon states (e.g. g^2 and g^3), and multiquark states ($q^2\overline{q}^2$, $q^4\overline{q}$, ...). Only a small fraction of these exotic states have been observed. Observation of these states, together with measurements of their masses and widths, and determination of their quantum numbers, is needed to compare to the predictions of lattice gauge theory, flux tube models, etc. The spectrum of $q\overline{q}$ mesons is well known below 1.5 GeV. Above 1.5 GeV the low angular momentum states are poorly known. This is the region where many exotic states are expected. For example, lattice gauge theory calculations predict Glue Balls with masses from 2 - 5 GeV. Our knowledge of the baryon spectrum is also incomplete. The only reasonably well-known excited light baryon state is the D(1232), whose properties are known to $\sim$ 5%. The properties of a few other excited states, the lowest in each partial wave, are known to 30%. Properties of other 'known' states have much larger uncertainties. Therefore higher precision information is needed and missing states must be sought in N$\pi\pi$, ΛK, ΣK scattering experiments. The nuclear physics community have invested heavily in experimental and theoretical programs aimed at better understanding QCD. The flagship DOE nuclear physics program for spectroscopy currently uses the electromagnetic beam facilities at JLab. However, since the production mechanisms for the various exotic states are not well understood, it is important to use different types of beam. Indeed, the electromagnetic probes available at JLab cannot be analyzed without accounting for the hadronic intermediate states. Hence, pion beam experiments at an upgraded Proton Driver would permit progress in light meson and hadron spectroscopy that would complement the JLab program. The measurements would also provide tests of lattice QCD, and are therefore of interest to the particle physics community. The beam and detector requirements for meson and baryon spectroscopy studies are quite modest. The low energy secondary pion and kaon beams derived from the 8 GeV primary proton beam would be used. A high duty cycle would be desirable, and hence a bunch stretcher would be required. For baryon spectroscopy, a secondary beam momentum of 2.5 GeV/c with π/K tagging (via a beam Cerenkov detector) is needed. This corresponds to a resonance mass of 2.37 (2.43) GeV/c^2 in the πp (Kp) system. A secondary beam momentum spread of 5% is adequate, but the beam momentum should be measured to 1%. The beam channel should be designed to focus the beam 3-5 meters downstream from the target. This allows room for 4π detectors and shielding. Attention should be paid to keeping backgrounds low, particularly for neutral particle detectors. Polarized targets will be needed, and recoil polarization measurements will be desirable.

4.4 Other Potential Opportunities

In addition to physics opportunities that exploit neutrino, muon, pion, and kaon beams, a high intensity Proton Driver might also support a variety of other experiments or using other secondary beams or using electrons (accelerated in the linac between H^- bunches, for example). Although all the possibilities have not been comprehensively explored, some specific examples using neutron beams and antiproton beams have been considered. These examples illustrate the long-term flexibility that a 2 MW Proton Driver would provide.

4.4.1 Neutrons

High power proton beams of a few GeV produce copious numbers of spallation neutrons in stopping targets. Dedicated neutron sources based on this production mechanism provide the highest peak neutron fluxes available for research purposes and provide time averaged fluxes that approach those available at the highest flux reactors. The primary scientific use for such sources lies in the application of neutrons in the thermal ($E \sim 25$ meV) and cold (1 meV $\leq E \leq$ 10 meV) regime for condensed matter research through the use of neutron scattering. In addition to this primary mission, spallation neutrons have research applications that transcend condensed matter research. Dedicated neutron scattering sources can address many of these auxiliary applications but there are others that, for a variety of reasons, are not appropriate at such facilities. A proton driver operating at 8 GeV and 2 MW would produce neutron beams with an intensity that is comparable to those from the most intense sources in the world. For many reasons including pulse structure, running time requirements, additional cost, as well as existing plans for comparable facilities, it is unlikely that the proton driver will be appropriate as a neutron source for neutron scattering. However, neutrons from production targets at the Proton Driver could be employed to support other types of experiment that will not be supported by next the generation of accelerator spallation sources. Potential opportunities include: 1) Production of Ultracold neutrons in a dedicated spallation target coupled to a superthermal converter, 2) Simulation of cosmic ray induced upsets of semiconductor devices, and 3) Search for neutron-antineutron oscillations. These experimental programs that are unlikely to be accommodated at the SNS or any other foreseen new facility. In more detail:

(i) **Ultracold Neutrons: Neutron Lifetime and Dipole Moment** Ultracold neutrons (UCN) are neutrons with sufficiently low kinetic energies that they can be confined in material or magnetic bottles. UCN have been used in a variety of important experiments including a search for the neutron electric dipole moment and the measurement of the neutron lifetime. Experiments of this nature are currently statistically limited by the intensity of existing UCN sources at high flux reactors. Recently a novel suggestion for the production of UCN using a spallation target has been undergoing tests at the Los Alamos Neutron Science Center (LANSCE) and elsewhere. The essence of the new method concerns the use of a small target that is very closely coupled to a solid

deuterium UCN converter. The inelastic scattering of low energy neutrons from a solid deuterium target at low temperature is dominated by phonon scattering. It has been shown that by exposing a solid deuterium target at low temperature (5K) to a cold or thermal neutron flux, it is possible to create an ensemble of UCN which is not in thermal equilibrium with the incident neutrons. In this way it is possible to significantly increase the density of UCN from that obtained in the traditional cryogenic moderators currently in use. Such a system has relatively modest beam requirements. Due to heating effects in the solid D_2, it is unlikely that such a source can be run at high duty cycle. At most, such a source at the Proton Driver would require 1 linac pulse every few tens of seconds. To accommodate the possibility for such a source at the Proton Driver, one would desire the provision of a pulsed beam switch that would allow the extraction of an occasional pulse and a suitable experimental area to accommodate the source and experimental equipment. The implementation of such a system could provide the US with a significant opportunity to establish a national UCN facility for a variety of scientific programs.

(ii) **Neutron-Antineutron Oscillations** Experimental searches for nucleon decay have so far produced only lower limits on the nucleon lifetime. These limits have excluded the simplest GUT models based on (B-L)-conserving SU(5) GUT and SUSY-GUT schemes. To make further progress, it is of considerable interest to extend the search for baryon number non-conservation beyond the simple proton decay experiments. An important candidate for such an extended search is the B = 2 neutron-antineutron transition. The oscillation of a free neutron into an antineutron can be studied in very controlled experimental conditions. The current limit on a possible transition time between the free neutron and antineutron is $\sim$ 108 s. This sensitivity is essentially statistics limited. Largely because there are no suitable sources available for a new experiment, there are, at present, no concrete plans to improve this result. The Proton Driver may provide the only opportunity for an improved measurement of a possible neutron-antineutron transition using free neutrons. A 2 MW Proton Driver could be designed to be a very efficient source of cold neutrons with average flux equivalent to that of the $\sim$ 20 MW research reactor. Such a source would consist of a stopping target that is neutronically coupled to a cryogenic cold moderator. This system should be of sufficient size to allow the extraction of a relatively large cross-section cold neutron beam. If such a source were optimized for an oscillation experiment, it is estimated that the current limit could be improved by 2-3 orders of magnitude.

(iii) **Cosmic-Ray Induced Semiconductor Upsets** As feature size in semiconductors gets smaller and the number of gates per chip becomes larger, the susceptibility of integrated circuits to radiation induced single errors increase. While it is well known that electronics in space may suffer disruptions from charged particles, it is less well known that cosmic ray induced upsets pose a non negligible issue for terrestrial electronics. At the Earth's surface and up to

aircraft altitudes it is cosmic ray induced neutrons rather than charged particles that are the principle source of upsets. Such neutron induced single-bit upsets and single-bit latch-ups are rare but in fact pose a problem to systems that require very high reliability (i.e. aircraft avionics) or in systems which require sustained operation of a very large number of gates (i.e. super computers). Indeed, this problem has received sufficient attention that the Joint Electron Device Engineering Council (JEDEC) has developed standards for the measurement of such upset rates. Because the comic ray induced production process is very similar to the spallation process, it is not surprising that the primary spectrum of spallation neutrons is very similar to that of cosmic ray induced neutrons. Indeed, accelerator based spallation neutron targets are the only sources that provide a spectrum of neutrons intense enough for the accelerated testing of semiconductors. However, it is important to note that spallation sources that are optimized for neutron scattering for materials science are designed for the extraction of only very low energy neutrons (typically a few meV?s). As a result, the beamlines at such facilities do not provide neutrons in the range of interest for single event upset tests (10-100 MeV). At present there is only one facility in world, the Weapons Neutron Research (WNR) facility at Los Alamos, that provides suitable beams. To accommodate the possibility of such a facility would require the provision for a beamline that would view a high current stopping target. A shutter and provision for an appropriately shielded irradiation facility would also be required.

4.4.2 Antiprotons

The antiproton source at Fermilab was designed and built to collect antiprotons for use at high energy in the Tevatron Collider. Although this is its primary use, in the past it has also been used to put stringent limits on the antiproton lifetime and, with a gas-jet target, to study charmonium states. It also provided the first unambiguous observation of atomic antihydrogen.

For the next several years the Tevatron Collider will operate at the highest possible luminosity and will therefore use all of the antiprotons that the antiproton source can provide. In the Proton Driver era, beyond collider operations, the Fermilab antiproton source could be exploited for other physics. At that time, there will exist only one, or possibly two, other antiproton sources in the world - one at GSI, and possibly one at CERN. The Fermilab source will likely be by far the most intense source of antiprotons in the world, especially because the Proton Driver is expected to improve the source intensity by up to a factor of two over the intensity expected at the end of Collider Run II. Thus Fermilab could host antiproton experiments with beam energies and/or intensities that are higher than those available elsewhere. Some examples of physics topics that might be of interest at a Proton Driver era antiproton source are:

(i) **Quarkononium Formation** The study of the charmonium and bottomonium systems has been crucial in unraveling the short-distance properties of the strong interaction. While most of the data have come from electron-positron interactions, a significant number of important measurements have been made in

studies of antiproton-proton formation of charmonium. Note that only 1^{--} states are directly formed by e^+e^- annihilation, although 0^{++} and 2^{++} states are formed in two-photon interactions. Other states must be studied in 1^{--} decays, yielding poor precision on masses and widths. Some of the most important states are difficult to reach in 1^{--} decays (e.g. 1^{+-} and 0^{+-} states). In particular the h_c and η_c' states are reported but unconfirmed, and the h_b, η_b and η_b' states are undiscovered. In $\bar{p}p$ formation all non-exotic mesons can be formed. Because of synchrotron radiation losses, the energy spread in e^+e^- colliders is large (several MeV). In an antiproton storage ring, the energy spread can be 10-100 keV allowing precise measurements of heavy- quarkonium masses and widths. Of potential interest to a Proton Driver era antiproton source program are: (a) In charmonium the h_c must be confirmed, the significant mass discrepancy between the BELLE and BABAR sightings of the η_c' resolved, the h_c and η_c' widths measured, and the other narrow states identified and characterized, namely the $\eta_{c2}(1^1D_2)$, $\psi_2(1^3D_2)[X(3872)?]$, 1^3D_3, 2^3P_2, and 1^1F_4. The interesting charmonium measurements could be made using a gas jet target in the Antiproton Accumulator, with a spectrometer similar to the E835 spectrometer. (b) In bottomonium the 1S, 2S, 1P and 2P singlet states are unobserved and the 1P and 2P χ_b masses have been measured at the 1 MeV level, but the widths are not yet measured. D states of bottomonium have not been observed. In order to study bottomonium, it will be necessary to build a new facility. The branching ratio of bottomonium states to $\overline{p}p$ have not yet been measured, so the formation cross section is unknown, but is expected to be small. The states are narrow, thus high luminosity and very small beam energy spread are required. We expect, for example χ_b formation cross sections to be no larger than $\sim$1 nb and χ_b widths to be $\sim$ 100 keV [119]. Therefore, the instantaneous luminosity should be at least 10^{32} cm^{-2}s^{-1} and the $s^{1/2}$ resolution $\sigma_E < 100$ keV. In the previous CERN and FNAL experiments, a hydrogen-gas-jet target intersected a high-current cooled stored $\bar{p}$ beam; E835 reached $L \sim 5 \times 10^{31}$ and $\sigma_E \sim 100$ keV at charmonium energies. A similar bottomonium experiment would require a $\bar{p}$ storage ring with variable energy between 46 and 56 GeV with $\Delta p/p \sim 10^{-5}$. An alternative design would be a symmetrical $\bar{p}p$ collider operating at 4.5-5.5 GeV per beam, again with $\Delta p/p \sim 10^{-5}$. It appears plausible to achieve the required luminosity. Such a machine could be designed to operate at charmonium energies at a smaller luminosity, which would be acceptable for that physics. We note that this machine would fit nicely into the Booster tunnel.

(ii) **CP Violation in Hyperon Decays** The Standard Model (SM) predicts a slight *CP* asymmetry in the decays of hyperons [120–126]. The most accessible signal, the fractional difference in the magnitudes of the α decay parameters [127] for a hyperon and its antiparticle [123,124,128,129], is predicted in the SM to be of order 10^{-5} for Λ decay [120–126]. In various extensions of the SM these can be much larger; for example, the supersymmetric calculation of He *et al.* [130] generates asymmetries as large as 1.9×10^{-3}. Sensitive measurements of hyperon and antihyperon decay can thus provide a new window into the underlying

mechanism of *CP* violation. Table 7 summarizes the experimental situation. The first three experiments cited studied Λ and $\overline{\Lambda}$ decay only [131–133]. Fermilab experiments E756 [134] and HyperCP (E871) [135–137] and CLEO [138] employed the cascade decay of charged Ξ and $\overline{\Xi}$ hyperons to produce polarized Λ's and $\overline{\Lambda}$'s, in whose subsequent decay the (anti)proton angular distribution measures the product of α_Ξ and α_Λ.

Expt.	Facility	Mode	A_Λ [*] or $A_{\Xi\Lambda}$ [†]	Ref.
R608	ISR	$pp \to \Lambda X, pp \to \overline{\Lambda} X$	$-0.02 \pm 0.14^*$	[131]
DM2	Orsay	$e^+e^- \to J/\psi \to \Lambda\overline{\Lambda}$	$0.01 \pm 0.10^*$	[132]
PS185	LEAR	$\overline{p}p \to \overline{\Lambda}\Lambda$	$0.006 \pm 0.015^*$	[133]
E756	FNAL	$pN \to \Xi^- X, \Xi^- \to \Lambda\pi^-$, $pN \to \overline{\Xi}^+ X, \overline{\Xi}^+ \to \overline{\Lambda}\pi^+$	$0.012 \pm 0.014^\dagger$	[134]
CLEO	CESR	$e^+e^- \to \Xi^- X, \Xi^- \to \Lambda\pi^-$, $e^+e^- \to \overline{\Xi}^+ X, \overline{\Xi}^+ \to \overline{\Lambda}\pi^+$	$-0.057 \pm 0.064 \pm 0.039^\dagger$	[138]
HyperCP‡	FNAL	$pN \to \Xi^- X, \Xi^- \to \Lambda\pi^-$, $pN \to \overline{\Xi}^+ X, \overline{\Xi}^+ \to \overline{\Lambda}\pi^+$	$(0.0 \pm 5.1 \pm 4.4) \times 10^{-4\dagger}$	[137]

‡Based on ≈5% of the total HyperCP dataset.

Table 7: Summary of experimental limits on *CP* violation in hyperon decay.

It is difficult to see how the HyperCP approach can be extrapolated to 10^{-5} sensitivity. However, the approach of PS185 may yet have significant "headroom" [139]. In 1992, Rapidis, et al. (P859) proposed to look for CP violation in the α parameter of Λ decay using the reaction $\overline{p}p \to \overline{\Lambda}\Lambda$ with a hydrogen gas jet target and a $\overline{p}$ beam energy of 1.641 GeV/c (above threshold for $\overline{\Lambda}\Lambda$ but below threshold for $\overline{\Lambda}\Sigma$). The experiment proposed building a small storage ring which could accept 3 GeV/c antiprotons from the Accumulator and decelerate them to the desired energy. The proponents of P859 estimated that they could reach a sensitivity of 10^{-4} in the fractional difference between the Λ and $\overline{\Lambda}$ α parameters in three months of running, consuming 6 mA of $\overline{p}$ current from the Accumulator per hour. Since 1992, the HyperCP experiment, which was also designed to study CP violation in hyperon decays (either Λ or Ξ) has been run. HyperCP has not yet published its final result, but it is likely that this experiment will achieve a sensitivity close to the 10^{-4} level that was the goal of P859. If systematics can be handled, it might be possible to reach the 10^{-5} level using the technique proposed by P859. This would require 100 times more events, but this sample could be collected in a few years, even assuming that the experiment used only one half of the total number of antiprotons provided by the antiproton source (assuming a stacking capacity of 80 mA/hour).

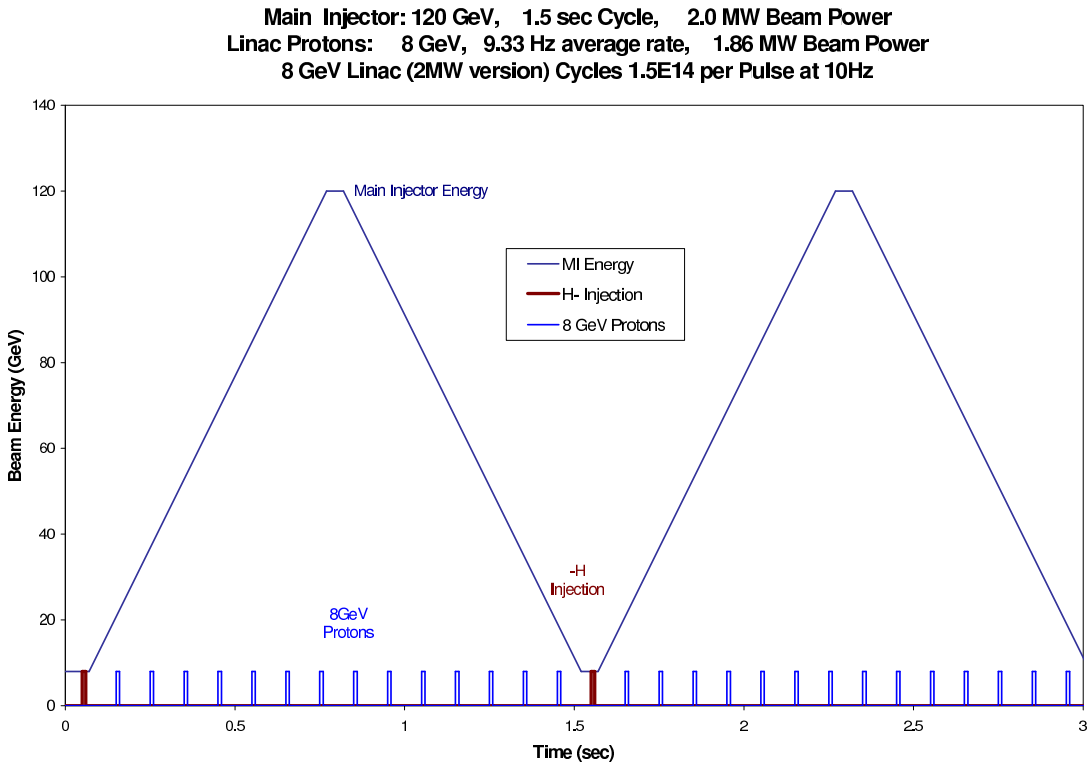

Figure 19: Proton Driver bunch structure and the Main Injector cycle.

5 Compatibilities and Proton Economics

The proton driver design that is currently favored consists of an 8 GeV H^- Linac that initially would produce a 0.5 MW beam, and that can eventually be upgraded to produce a 2 MW beam. A small fraction of the 8 GeV beam would be used to fill the MI with the maximum beam that, with some modest improvements, it can accelerate. This would yield a 2 MW beam at MI energies. Hence the upgraded proton source would deliver two beams that can be simultaneously used for experiments: a 2 MW beam at MI energies, and eventually an almost 2 MW beam at 8 GeV. To illustrate this the cycle structure is shown in Fig. 19. The MI would receive one pulse from the Linac every 1.5 sec. The cycle time is dominated by the time to ramp up and ramp down the MI energy. The 14 Linac pulses that are available, whilst the MI is ramping and at flat top, would provide beam for an 8 GeV program.

The initial NUE long-baseline program would be expected to be the primary user of the 2 MW MI beam. The high-energy neutrino scattering program also needs this beam, and would be expected to coexist with NUE. The other candidate uses of the MI beam include supporting experiments at an antiproton source, and supporting a kaon experiments. The antiproton source could operate in parallel with the MI neutrino program with a modest reduction in the available POT for the NuMI beam. The kaon program, in contrast to the neutrino program, would require a slowly extracted beam. However, with an additional storage ring, it is possible that a kaon program

could be run during neutrino running with only a minor impact on the POT available for the neutrino program. This could be accomplished by fast extraction of a fraction of the MI bunches and transfer into a stretcher ring. The protons stored in the ring would then be slowly extracted for the kaon program. A ring in the Tevatron tunnel would be ideal for this purpose.

The candidates for using the 8 GeV beam are a low energy neutrino scattering experiment, a pion program, a muon program, and a neutron program. The neutrino scattering experiment requires short pulses with large gaps between pulses so that beam-unrelated backgrounds can be suppressed. The pion program requires a beam stretcher to produce long pulses and hence minimize the instantaneous intensity. Many experiments in the muon program require a CW beam with bunches that are short compared to the muon lifetime with gaps between bunches of several muon lifetimes. Hence all of these programs will require an additional storage ring to manipulate the bunch structure. It is possible that, in the post-collider era, this storage ring could be the Recycler. Noting that each of these 8 GeV sub-programs requires a different bunch structure it is natural to consider a scenario in which they run sequentially rather than in parallel. To illustrate this, we can imagine that initially an 8 GeV neutrino scattering experiment is the primary user of the 8 GeV beam, followed by (or possibly interleaved with) one or more pion experiments. In a second phase the facility is upgraded to include a low energy muon source, and one or more low energy muon experiments become the primary user(s). In a third phase, if required, the muon source could be developed to become the front-end of a neutrino factory. This could be a very long-term 20 - 30 year plan.

6 Summary

There appears to be a compelling physics case for a new Proton Driver at Fermilab. This upgrade to the existing accelerator complex is motivated by the exciting developments in neutrino physics. Independent of the value of the unknown neutrino mixing parameter θ_{13}, a 2 MW Main Injector proton beam would facilitate, over the coming decades, one or more long-baseline neutrino experiments that would make critical contributions to the global neutrino oscillation program. The MI neutrino oscillation physics program would be supplemented with a broad program of neutrino scattering measurements that are of interest to particle physicists, nuclear physicists, and nuclear astrophysicists. The neutrino scattering program would utilize both the Proton Driver upgraded NUMI beam, and neutrino and antineutrino beams generated using the protons available at 8 GeV. The overall neutrino program motivates the highest practical primary beam intensities at both MI energies and at 8 GeV. In practice this means 2 MW at MI energies and 0.5-2 MW at 8 GeV.

Additional physics programs could also be supported by the Proton Driver. In particular, the Proton Driver could support (i) a program of low energy experiments that probe the TeV mass scale in a way that is complementary to the LHC experiments, and (ii) a program of low energy experiments that are of interest to the nuclear physics community and that is complementary to the JLab program. The possibilities using

the 8 GeV beam include (i) the development of a very intense muon source with a bunch structure optimized for (g-2), muon EDM, and LFV muon decay experiments, (ii) a program of low energy pion experiments, and (iii) some specific experiments using spallation neutrons. The possibilities using the MI beam include a program of kaon experiments, and some specific experiments using the antiproton source.

Thus, an upgraded proton source would support, for decades to come, an exciting world class neutrino program running in parallel with a broader program of low energy experiments.

DRAFT

References

[1] Y. Fukuda *et al.* (Kamiokande), Phys. Lett. **B335**, 237 (1994).

[2] Y. Fukuda *et al.* (Super-Kamiokande), Phys. Rev. Lett. **81**, 1562 (1998), hep-ex/9807003.

[3] S. Fukuda *et al.* (Super-Kamiokande), Phys. Rev. Lett. **85**, 3999 (2000), hep-ex/0009001.

[4] S. H. Ahn *et al.* (K2K), Phys. Lett. **B511**, 178 (2001), hep-ex/0103001.

[5] M. H. Ahn *et al.* (K2K), Phys. Rev. Lett. **90**, 041801 (2003), hep-ex/0212007.

[6] M. Apollonio *et al.* (CHOOZ), Phys. Lett. **B466**, 415 (1999), hep-ex/9907037.

[7] Q. R. Ahmad *et al.* (SNO), Phys. Rev. Lett. **87**, 071301 (2001), nucl-ex/0106015.

[8] S. N. Ahmed *et al.* (SNO), Phys. Rev. Lett. **92**, 181301 (2004), nucl-ex/0309004.

[9] S. Fukuda *et al.* (Super-Kamiokande), Phys. Lett. **B539**, 179 (2002), hep-ex/0205075.

[10] K. Eguchi *et al.* (KamLAND), Phys. Rev. Lett. **90**, 021802 (2003), hep-ex/0212021.

[11] J. N. Bahcall, M. C. Gonzalez-Garcia, and C. Pena-Garay, JHEP **08**, 016 (2004), hep-ph/0406294.

[12] A. Bandyopadhyay, S. Choubey, S. Goswami, S. T. Petcov, and D. P. Roy (2004), hep-ph/0406328.

[13] M. Maltoni, T. Schwetz, M. A. Tortola, and J. W. F. Valle (2004), hep-ph/0405172.

[14] A. Aguilar *et al.* (LSND), Phys. Rev. **D64**, 112007 (2001), hep-ex/0104049.

[15] E. Church *et al.* (BooNe) FERMILAB-PROPOSAL-0898.

[16] P. Minkowski, Phys. Lett. **B67**, 421 (1977).

[17] T. Yanagida, in *Proceedings of the Workshop on the Unified Theory and the Baryon Number in the Universe*, edited by O. Sawada and A. Sugamoto (KEK, Tsukuba, Japan, 1979), p. 95.

[18] S. L. Glashow, in *Proceedings of the 1979 Cargèse Summer Institute on Quarks and Leptons*, edited by M. Lévy, J.-L. Basdevant, D. Speiser, J. Weyers, R. Gastmans, and M. Jacob (Plenum Press, New York, 1980), pp. 687–713.

[19] M. Gell-Mann, P. Ramond, and R. Slansky, in *Supergravity*, edited by P. van Nieuwenhuizen and D. Z. Freedman (North Holland, Amsterdam, 1979), p. 315.

[20] R. N. Mohapatra and G. Senjanović, Phys. Rev. Lett. **44**, 912 (1980).

[21] N. Arkani-Hamed, L. J. Hall, H. Murayama, D. R. Smith, and N. Weiner, Phys. Rev. **D64**, 115011 (2001), hep-ph/0006312.

[22] F. Borzumati and Y. Nomura, Phys. Rev. **D64**, 053005 (2001), hep-ph/0007018.

[23] R. Kitano, Phys. Lett. **B539**, 102 (2002), hep-ph/0204164.

[24] R. Arnowitt, B. Dutta, and B. Hu, Nucl. Phys. **B682**, 347 (2004), hep-th/0309033.

[25] S. Abel, A. Dedes, and K. Tamvakis (2004), hep-ph/0402287.

[26] H. S. Goh, R. N. Mohapatra, and S.-P. Ng, Phys. Rev. **D68**, 115008 (2003), hep-ph/0308197.

[27] T. Asaka, W. Buchmüller, and L. Covi, Phys. Lett. **B563**, 209 (2003), hep-ph/0304142.

[28] K. S. Babu, J. C. Pati, and F. Wilczek, Nucl. Phys. **B566**, 33 (2000), hep-ph/9812538.

[29] C. H. Albright and S. M. Barr, Phys. Rev. **D64**, 073010 (2001), hep-ph/0104294.

[30] T. Blazek, S. Raby, and K. Tobe, Phys. Rev. **D62**, 055001 (2000), hep-ph/9912482.

[31] G. G. Ross and L. Velasco-Sevilla, Nucl. Phys. **B653**, 3 (2003), hep-ph/0208218.

DRAFT

[32] S. Raby, Phys. Lett. **B561**, 119 (2003), hep-ph/0302027.

[33] R. Kitano and Y. Mimura, Phys. Rev. **D63**, 016008 (2001), hep-ph/0008269.

[34] N. Maekawa, Prog. Theor. Phys. **106**, 401 (2001), hep-ph/0104200.

[35] M.-C. Chen and K. T. Mahanthappa, Phys. Rev. **D68**, 017301 (2003), hep-ph/0212375.

[36] M. Bando and M. Obara, Prog. Theor. Phys. **109**, 995 (2003), hep-ph/0302034.

[37] W. Buchmüller and D. Wyler, Phys. Lett. **B521**, 291 (2001), hep-ph/0108216.

[38] P. H. Frampton and R. N. Mohapatra (2004), hep-ph/0407139.

[39] W. Grimus and L. Lavoura, JHEP **07**, 045 (2001), hep-ph/0105212.

[40] W. Grimus and L. Lavoura, Phys. Lett. **B572**, 189 (2003), hep-ph/0305046.

[41] W. Grimus, A. S. Joshipura, S. Kaneko, L. Lavoura, and M. Tanimoto, JHEP **07**, 078 (2004), hep-ph/0407112.

[42] S.-L. Chen, M. Frigerio, and E. Ma (2004), hep-ph/0404084.

[43] I. Aizawa, M. Ishiguro, T. Kitabayashi, and M. Yasue, Phys. Rev. **D70**, 015011 (2004), hep-ph/0405201.

[44] R. N. Mohapatra, JHEP **10**, 027 (2004), hep-ph/0408187.

[45] S. Antusch and S. F. King (2004), hep-ph/0402121.

[46] S. Antusch and S. F. King, Phys. Lett. **B591**, 104 (2004), hep-ph/0403053.

[47] W. Rodejohann and Z.-z. Xing (2004), hep-ph/0408195.

[48] K. S. Babu, E. Ma, and J. W. F. Valle, Phys. Lett. **B552**, 207 (2003), hep-ph/0206292.

[49] T. Ohlsson and G. Seidl, Nucl. Phys. **B643**, 247 (2002), hep-ph/0206087.

[50] S. F. King and G. G. Ross, Phys. Lett. **B574**, 239 (2003), hep-ph/0307190.

[51] Q. Shafi and Z. Tavartkiladze, Phys. Lett. **B594**, 177 (2004), hep-ph/0401235.

[52] M. Bando, S. Kaneko, M. Obara, and M. Tanimoto, Phys. Lett. **B580**, 229 (2004), hep-ph/0309310.

[53] M. Honda, S. Kaneko, and M. Tanimoto, JHEP **09**, 028 (2003), hep-ph/0303227.

[54] R. F. Lebed and D. R. Martin, Phys. Rev. **D70**, 013004 (2004), hep-ph/0312219.

[55] A. Ibarra and G. G. Ross, Phys. Lett. **B575**, 279 (2003), hep-ph/0307051.

[56] P. F. Harrison and W. G. Scott, Phys. Lett. **B594**, 324 (2004), hep-ph/0403278.

[57] P. H. Frampton, S. L. Glashow, and T. Yanagida, Phys. Lett. **B548**, 119 (2002), hep-ph/0208157.

[58] J.-w. Mei and Z.-z. Xing, Phys. Rev. **D69**, 073003 (2004), hep-ph/0312167.

[59] A. de Gouvea and H. Murayama, Phys. Lett. **B573**, 94 (2003), hep-ph/0301050.

[60] R. N. Mohapatra, M. K. Parida, and G. Rajasekaran, Phys. Rev. **D69**, 053007 (2004), hep-ph/0301234.

[61] S. Antusch, J. Kersten, M. Lindner, and M. Ratz, Nucl. Phys. **B674**, 401 (2003), hep-ph/0305273.

[62] P. H. Chankowski, W. Krolikowski, and S. Pokorski, Phys. Lett. **B473**, 109 (2000), hep-ph/9910231.

DRAFT

[63] J. A. Casas, J. R. Espinosa, A. Ibarra, and I. Navarro, Nucl. Phys. **B573**, 652 (2000), hep-ph/9910420.

[64] M.-C. Chen and K. T. Mahanthappa, Int. J. Mod. Phys. **A18**, 5819 (2003), hep-ph/0305088.

[65] G. Altarelli and F. Feruglio (2004), hep-ph/0405048.

[66] S. T. Petcov, Phys. Lett. **B110**, 245 (1982).

[67] C. N. Leung and S. T. Petcov, Phys. Lett. **B125**, 461 (1983).

[68] M. Fukugita and T. Yanagida, Phys. Lett. **174B**, 45 (1986).

[69] G. C. Branco, T. Morozumi, B. M. Nobre, and M. N. Rebelo, Nucl. Phys. **B617**, 475 (2001), hep-ph/0107164.

[70] S. Pascoli, S. T. Petcov, and W. Rodejohann, Phys. Rev. **D68**, 093007 (2003), hep-ph/0302054.

[71] S. F. King, Phys. Rev. **D67**, 113010 (2003), hep-ph/0211228.

[72] J. C. Pati (2002), hep-ph/0209160.

[73] P. F. Harrison and W. G. Scott, Phys. Lett. **B557**, 76 (2003), hep-ph/0302025.

[74] J. Kubo, Phys. Lett. **B578**, 156 (2004), hep-ph/0309167.

[75] E. Ma, Mod. Phys. Lett. **A19**, 577 (2004), hep-ph/0401025.

[76] M. Raidal (2004), hep-ph/0404046.

[77] S. F. King, Nucl. Phys. **B576**, 85 (2000), hep-ph/9912492.

[78] S. F. King, JHEP **09**, 011 (2002), hep-ph/0204360.

[79] S. Antusch and S. F. King (2004), hep-ph/0405272.

[80] G. G. Ross, L. Velasco-Sevilla, and O. Vives, Nucl. Phys. **B692**, 50 (2004), hep-ph/0401064.

[81] S. Zhou and Z.-z. Xing (2004), hep-ph/0404188.

[82] P. H. Frampton, S. T. Petcov, and W. Rodejohann, Nucl. Phys. **B687**, 31 (2004), hep-ph/0401206.

[83] W. Rodejohann (2004), hep-ph/0403236.

[84] A. de Gouvêa, Phys. Rev. **D69**, 093007 (2004), hep-ph/0401220.

[85] T. Appelquist and R. Shrock, Phys. Lett. **B548**, 204 (2002), hep-ph/0204141.

[86] J. A. Casas, J. R. Espinosa, and I. Navarro, JHEP **09**, 048 (2003), hep-ph/0306243.

[87] I. Dorsner and A. Y. Smirnov, Nucl. Phys. **B698**, 386 (2004), hep-ph/0403305.

[88] P. Huber, M. Lindner, M. Rolinec, T. Schwetz, and W. Winter, Phys. Rev. **D70**, 073014 (2004), hep-ph/0403068.

[89] G. L. Fogli, E. Lisi, A. Marrone, and D. Montanino, Phys. Rev. **D67**, 093006 (2003), hep-ph/0303064.

[90] M. Maltoni, T. Schwetz, M. A. Tortola, and J. W. F. Valle, Phys. Rev. **D68**, 113010 (2003), hep-ph/0309130.

[91] Y. f. t. S.-K. C. Hayato, talk given at the HEP2003 conference (Aachen, Germany, 2003), http://eps2003.physik.rwth-aachen.de.

[92] F. Ardellier *et al.* (2004), hep-ex/0405032.

[93] P. Huber, M. Lindner, and W. Winter, Nucl. Phys. **B645**, 3 (2002), hep-ph/0204352.

DRAFT

[94] M. V. Diwan (2004), hep-ex/0407047.

[95] D. A. Harris *et al.* (Minerva) MINERνA Note 800, September, 2004, arXiv:hep-ex/0410010.

[96] B. Portheault (2004), hep-ph/0406226.

[97] M. Botje, Euro. Phys. Jour. C **14**, 285 (2000).

[98] X. Ji, Phys. Rev. Lett. p. 610 (1997).

[99] X. Ji, Phys. Rev. **D55**, 7114 (1997).

[100] A. Radyushkin, Phys. Lett. **B380**, 417 (1996).

[101] A. Radyushkin, Phys. Lett. **B385**, 333 (1996).

[102] J. Collins, L. Frankfurt, and M. Strikman, Phys. Rev. **D56**, 2982 (1997).

[103] Private communcation.

[104] B. Filippone and X. Ji, Adv. Nucl. Phys. **26**, 1 (2001), hep-ph/0101224.

[105] L. Auerbach *et al.*, Phys. Rev. D **63**, 112001 (2001), hep-ex/0101039.

[106] M. Jones *et al.*, Phys. Rev. Lett **84**, 1398 (2000).

[107] O. Gayou *et al.*, Phys. Rev. Lett **88**, 092301 (2002).

[108] I. Niculescu *et al.*, Phys. Rev. Lett. **85**, 1182 (2000).

[109] W. Melnitchouk, R. Ent, and C. Keppel Accepted by Physics Reports.

[110] S. Jeschonnek and J. Van Orden, Phys. Rev. **D69**, 054006 (2004).

[111] F. Close and N. Isgur, Phys. Lett. **B509**, 81 (2001).

[112] R. Ent, C. Keppel, and I. Niculescu, Phys. Rev. **D62**, 073008 (2000).

[113] C. Carlson and N. Mukhopadhyay, Phys. Rev. **D47**, 1737 (1993).

[114] M. Diemoz, F. Ferroni, and E. Longo, Phys. Rev. **130**, 293 (1986).

[115] R. Belusevic and D. Rein, Phys. Rev. **D38**, 2753 (1988).

[116] R. Belusevic and D. Rein, Phys. Rev. **D46**, 3747 (1992).

[117] R. Shrock, Phys. Rev. **D12**, 2049 (1975).

[118] A. Amer, Phys. Rev. **D18**, 2290 (1978).

[119] B. Ioffe, Phys. Rev. **47**, 340 (1993).

[120] A. Pais, Phys. Rev. Lett. **3**, 242 (1959).

[121] Q. Overseth and S. Pakvasa, Phys. Rev. **184**, 1663 (1969).

[122] J. Donoghue and S. Pakvasa, Phys. Rev. Lett. **55**, 162 (1985).

[123] J. Donoghue, X. He, and S. Pakvasa, Phys. Rev. **D34**, 833 (1986).

[124] X. He, H. Steger, and G. Valencia, Phys. Lett. **B272**, 411 (1991).

[125] G. Valencia Proc. $\overline{p}$2000 Workshop, *op cit.*

[126] J. Tandean and G. Valencia, Phys. Rev. **D67**, 056001 (2003).

[127] T. Lee and C. Yang, Phys. Rev. **108**, 1645 (1957).

[128] J. Donoghue, B. Holstein, and G. Valencia, Phys. Lett. **178B**, 319 (1986).

[129] J. Donoghue, B. Holstein, and G. Valencia, Int. J. Mod. Phys. **A2**, 319 (1987).

[130] X. He, H. Murayama, S. Pakvasa, and G. Valencia, Phys. Rev. **D61**, 071701(R) (2000).

DRAFT

[131] P. Chauvat *et al.*, Phys. Lett. **163B**, 273 (1985).

[132] M. Tixier *et al.*, Phys. Lett. **B212**, 523 (1988).

[133] P. Barnes *et al.*, Nucl. Phys. B (Proc. Suppl.) **56A**, 46 (1997).

[134] K. Luk *et al.*, Phys. Rev. Lett. **85**, 4860 (2000).

[135] J. Antos *et al.* (1994).

[136] R. Burnstein *et al.* To appear in Nucl. Instrum. Methods (2004), `hep-ex/0405034`, URL `http://ppd.fnal.gov/experiments/e871/welcome.html`.

[137] T. Holmstrom *et al.*, Phys. Rev. Lett. **93**, 262001 (2004).

[138] D. Jaffe *et al.* (2000), cLNS 98/1587, CLEO 98-16, `hep-ex/0009037`.

[139] D. Kaplan, Nucl. Phys. **A692**, 206 (2001), in Proc. Biennial Conf. on Low-Energy Antiproton Physics (LEAP 2000), Venice, Italy, 20–26 Aug 2000.

DRAFT